



中国生态大讲堂冬季研讨会

Dec 21, 2008

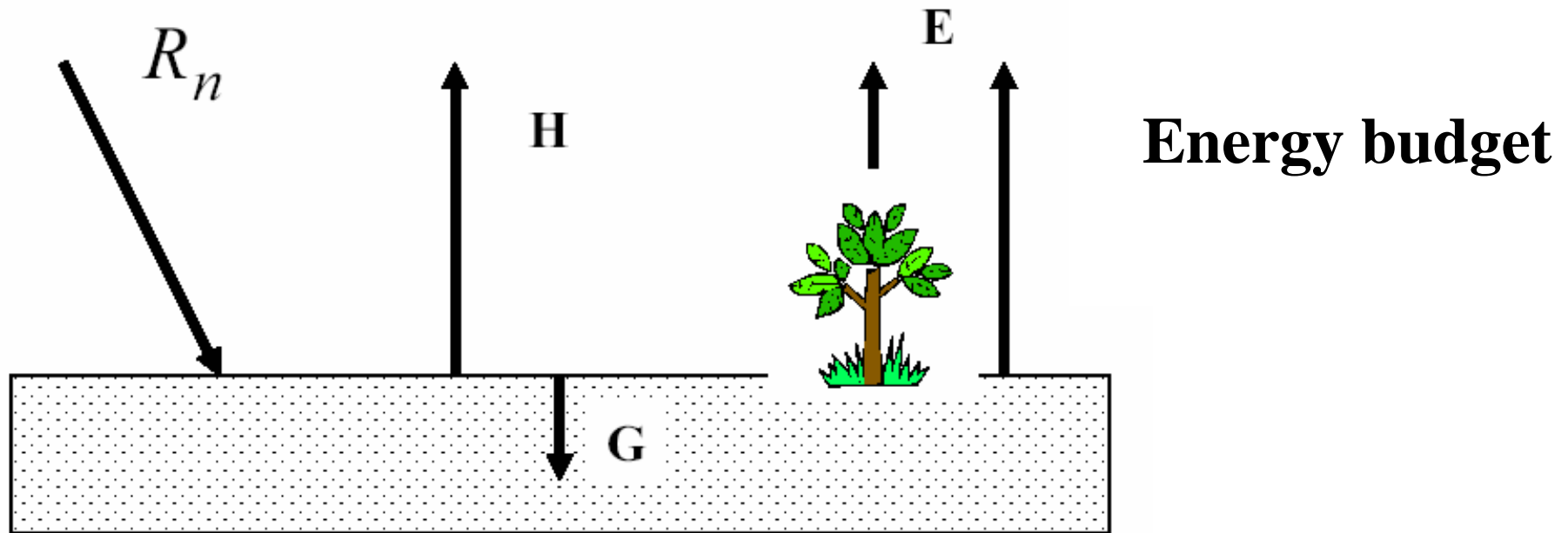
利用卫星数据估算地表辐射及能量通量的研究新进展

梁顺林, Professor

Department of Geography

University of Maryland at College Park, USA

Sliang@geog.umd.edu, <http://www.glue.umd.edu/~sliang>



$$R_n = R_n^s + R_n^l = (1 - \alpha)F_d^s + \varepsilon F_d^l - \sigma \varepsilon T^4$$

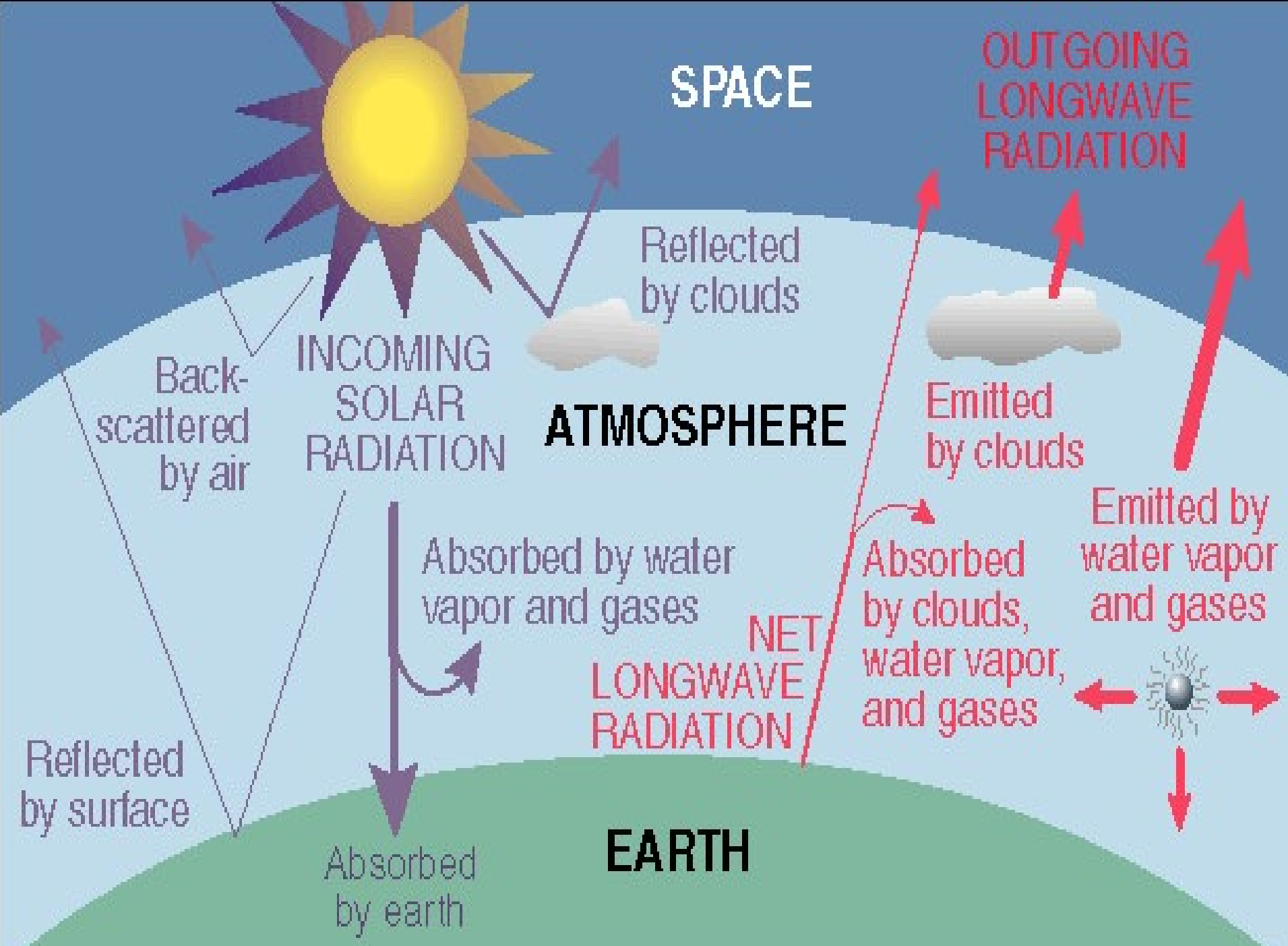
Annotations for the equation terms:

- R_n^s : albedo
- F_d^s : Insolation
- εF_d^l : Longwave downward radiation
- $\sigma \varepsilon T^4$: Emissivity
Skin temperature

Radiation budget



UNIVERSITY OF
MARYLAND



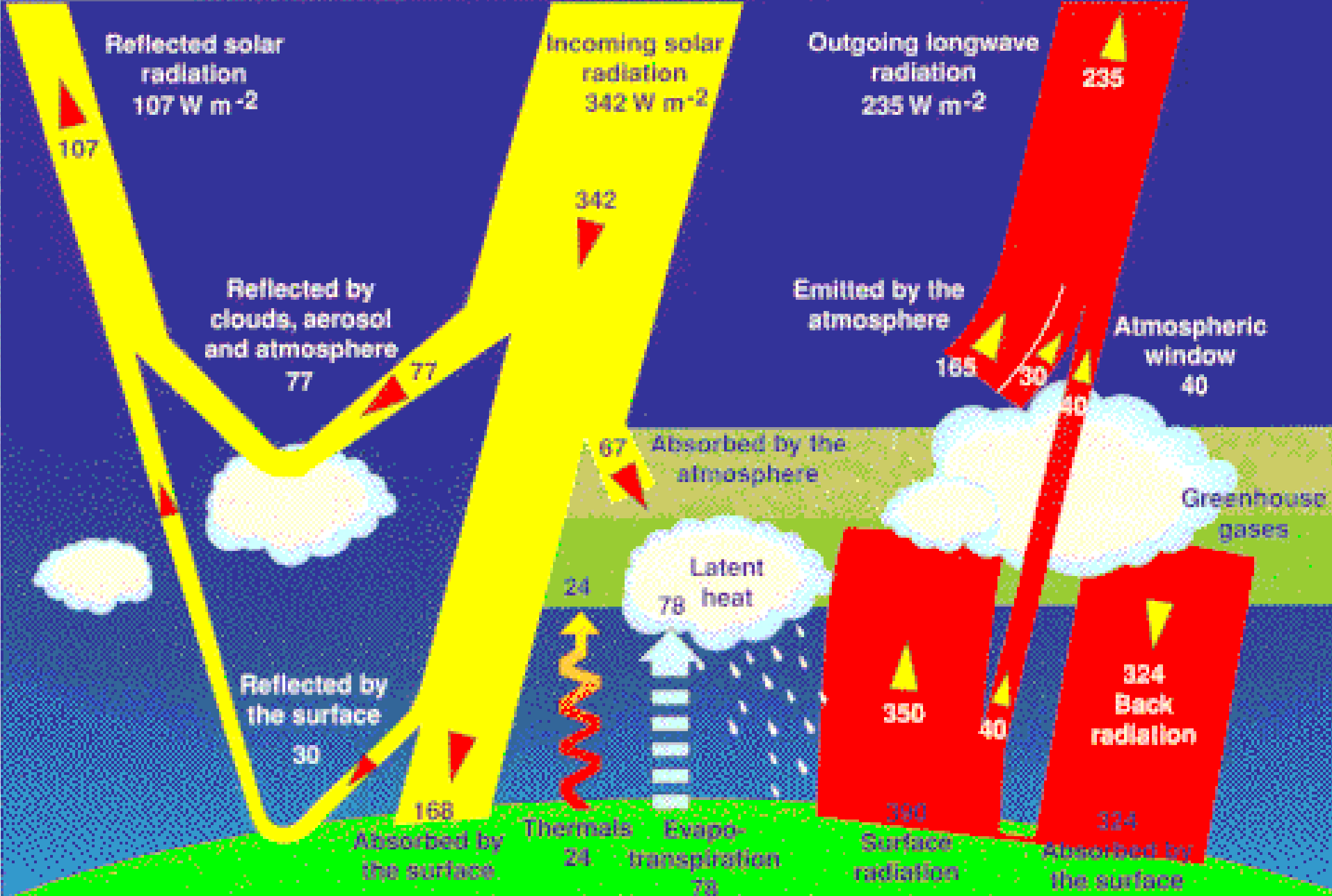
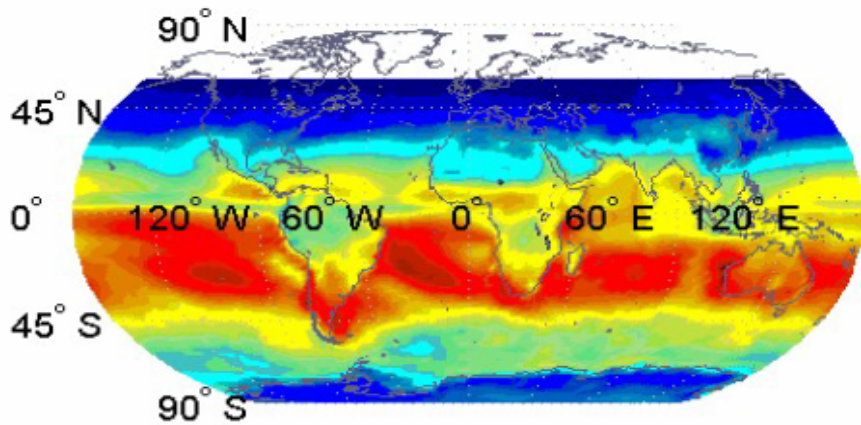
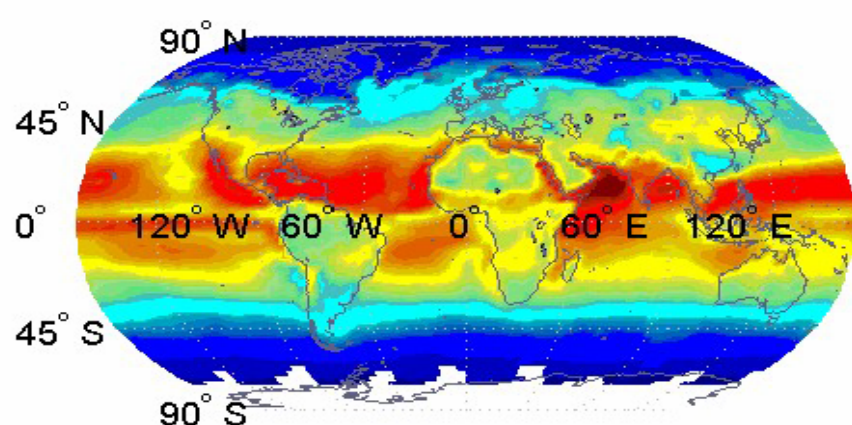
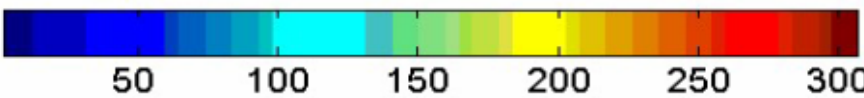


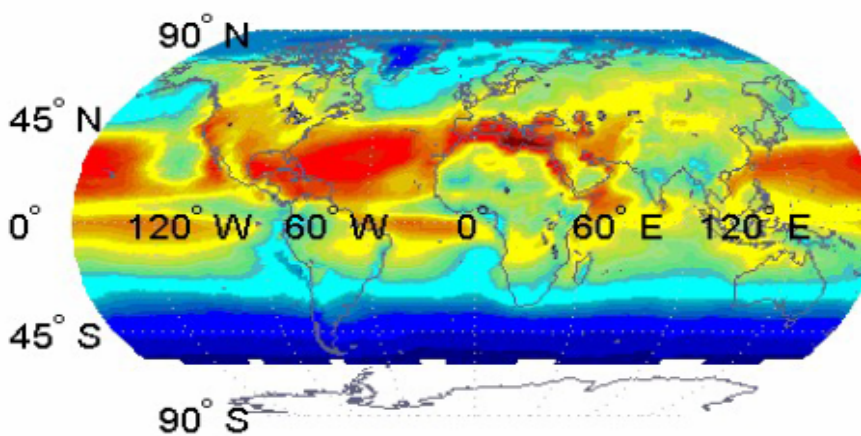
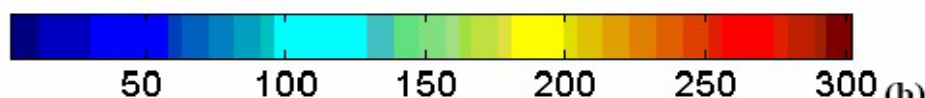
Figure Courtesy:<http://asd-www.larc.nasa.gov/ceres/brochure> based on data from [Kiehl and Trenberth \(1997\)](#)



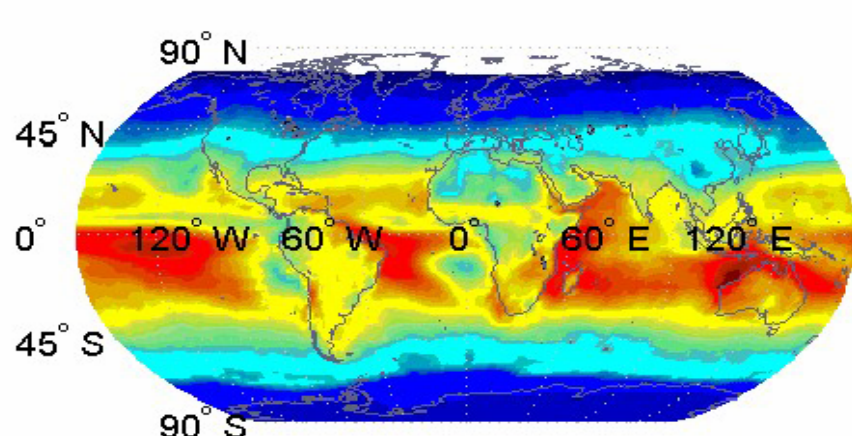
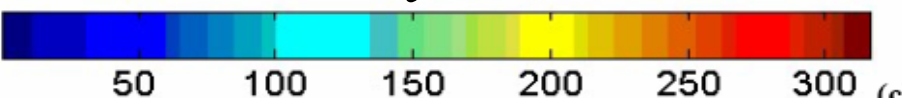
Jan.



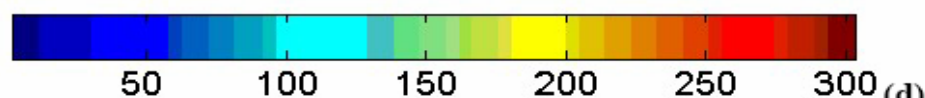
April



July

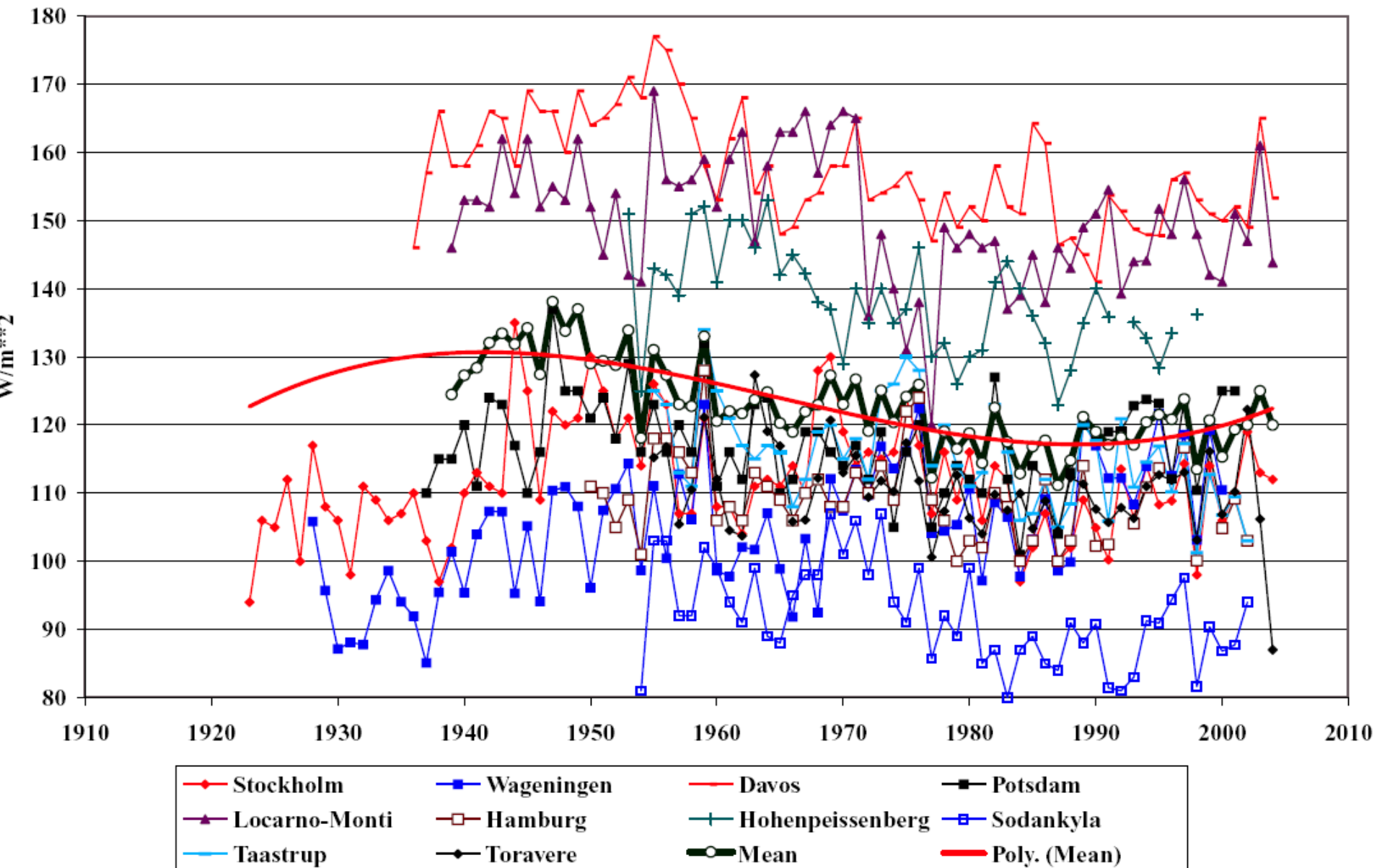


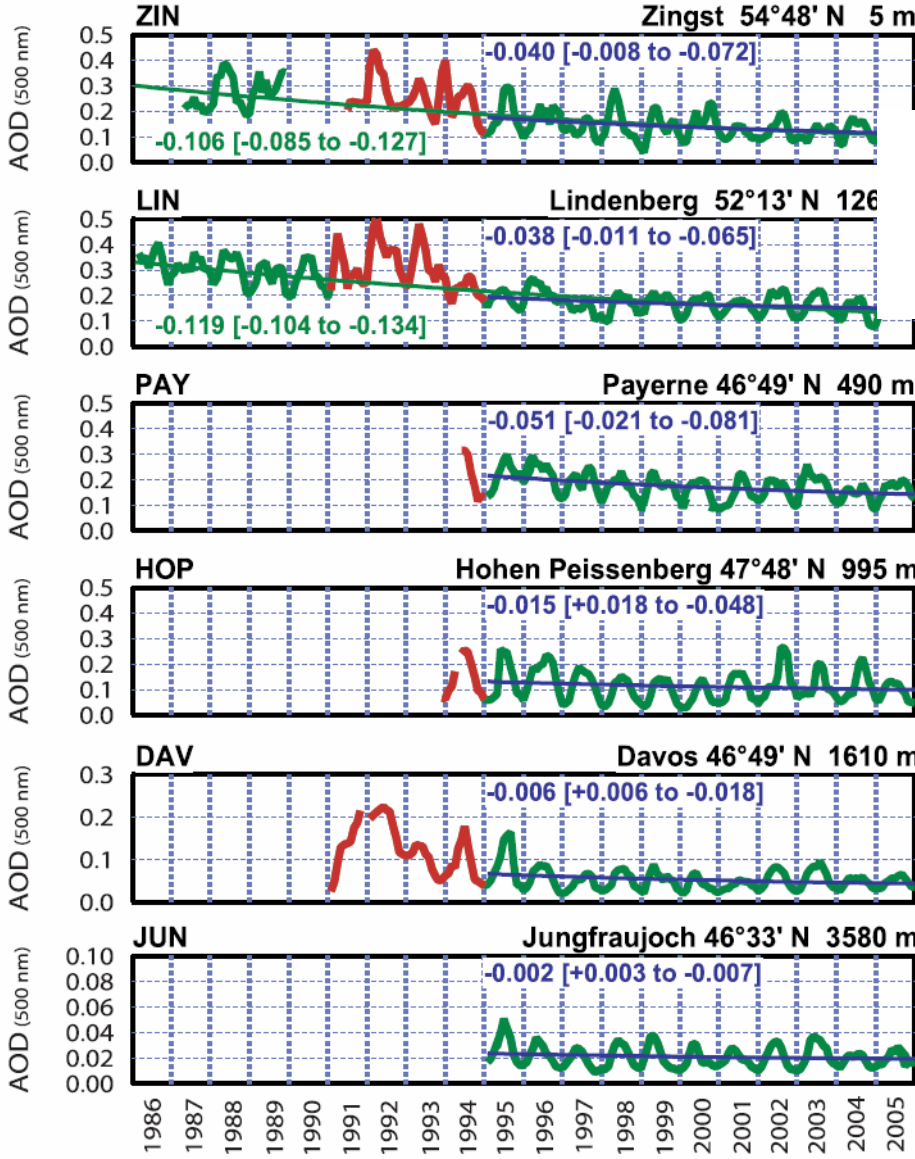
Oct.



Long-term (1984–2000) average global distribution of net surface shortwave radiation (Wm⁻²)
(Hatzianastassiou et al., 2005)

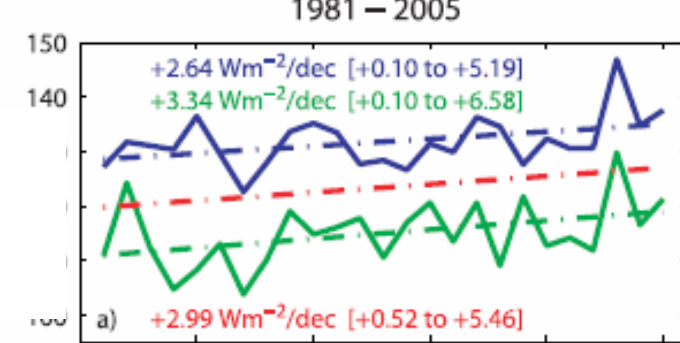
Global radiation for Europe for sites with more than 50 years observation





Aerosol optical depth, radiation, temperature measured in German & Switzerland, Ruckstuhl et al. (2008)

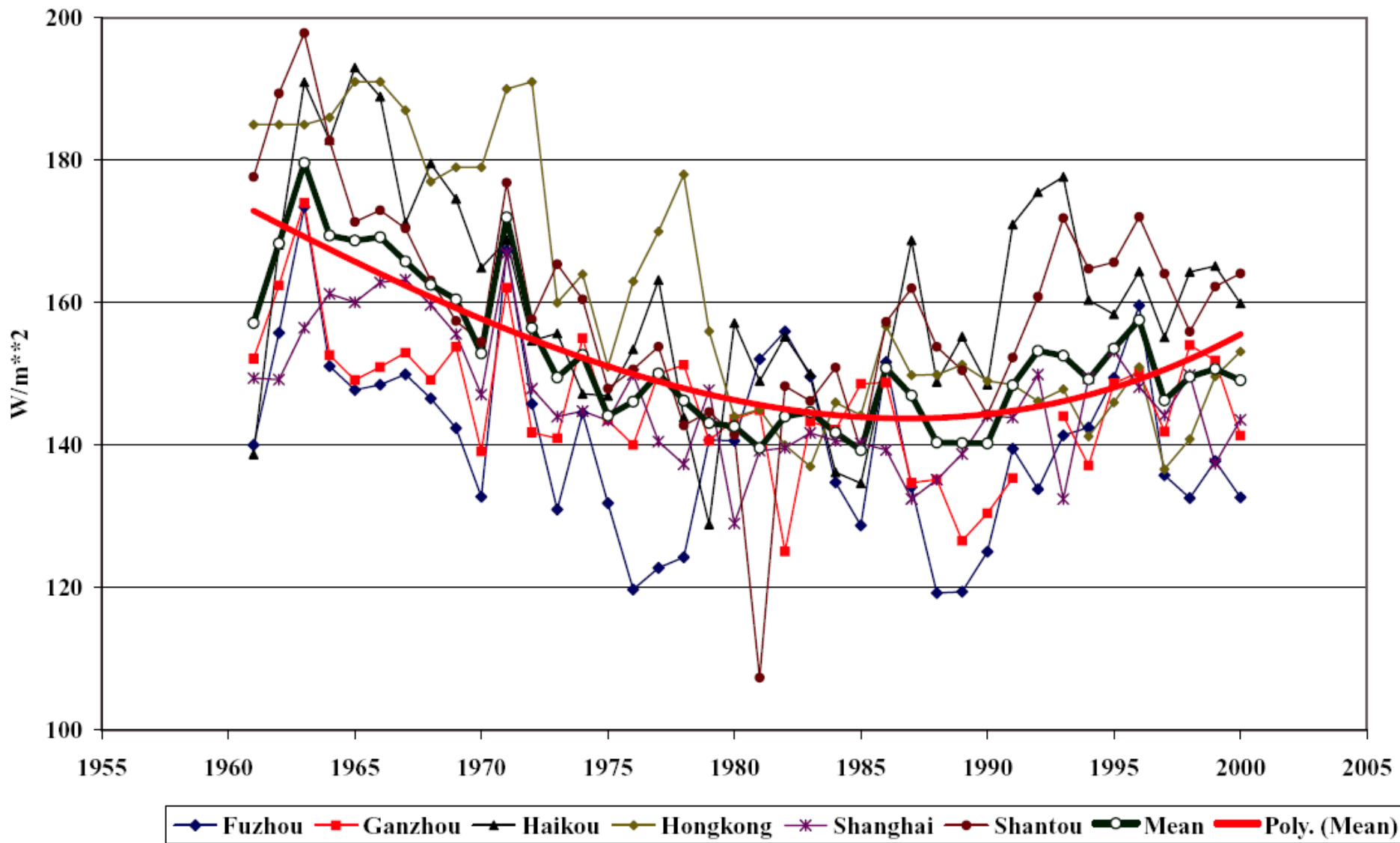
Total insolation



Clear-sky

Cloudy-sky

Best 6 stations in southeast China



UNIVERSITY OF
MARYLAND

Table 2. Relative Average Increment (AI, $AI = (y - x)/x$)^a

Sites	Evaporative Fraction			Light-Use Efficiency		
	$R_d/R_s: 0.2 - 0.4$	$R_d/R_s: 0.4 - 0.8$	$R_d/R_s: 0.8 - 1.0$	$R_d/R_s: 0.2 - 0.4$	$R_d/R_s: 0.4 - 0.8$	$R_d/R_s: 0.8 - 1.0$
E01	0.104	0.151	0.127	-0.064	0.169	2.191
E03	0.161	0.124	0.180	0.007	0.229	1.772
E05	0.138	0.174	0.221	-0.094	0.184	2.181
E06	0.119	0.122	0.233	0.000	0.221	1.845
E10	0.139	0.154	0.208	-0.029	0.356	2.031
E14	0.198	0.244	0.267	-0.098	0.068	1.452
E16	0.216	0.286	0.346	-0.107	0.118	1.889
E21	0.150	0.158	0.209	-0.055	0.241	2.720
E24	0.158	0.198	0.305	-0.077	0.161	2.169
Mean	0.154	0.179	0.232	-0.057	0.194	2.028
RMSE	0.036	0.055	0.066	0.0420	0.082	0.354

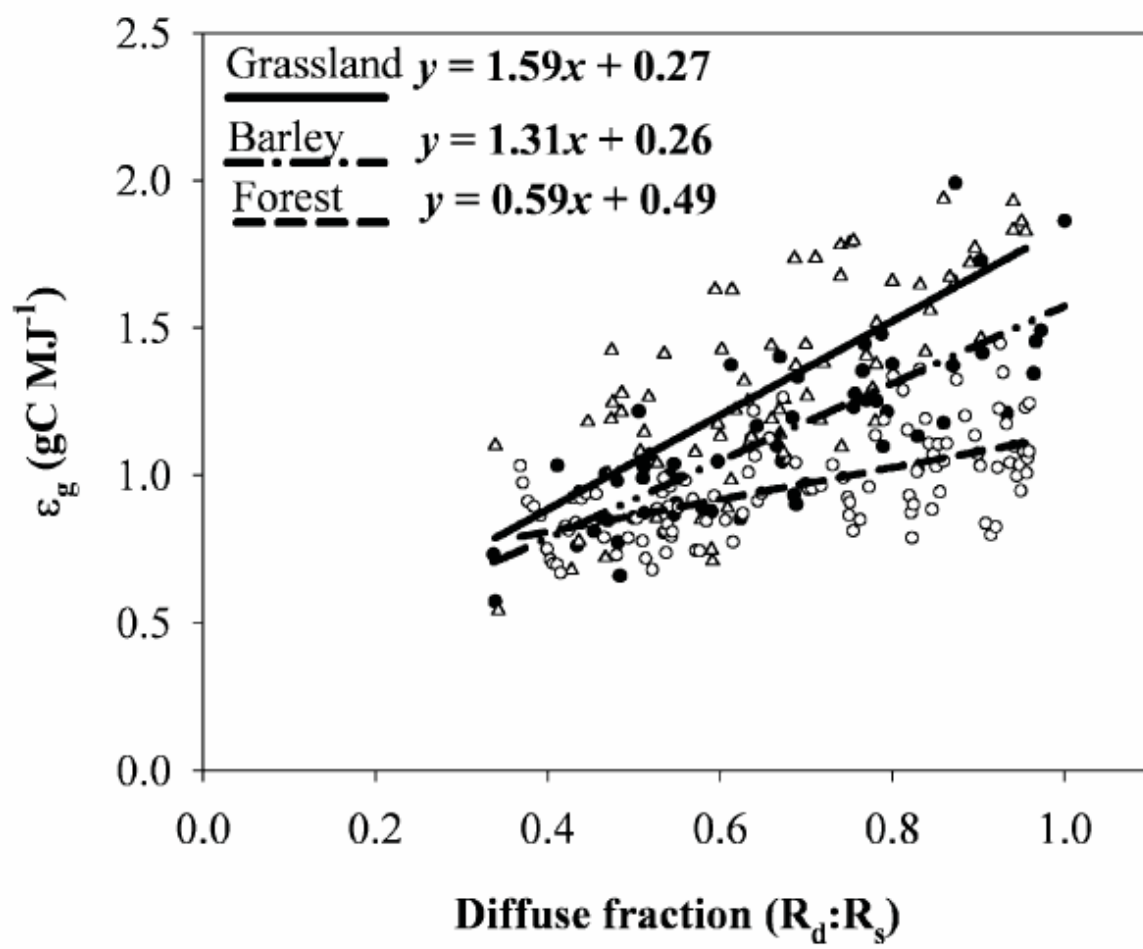
^aHere x is either EF or LUE within an R_d/R_s interval and Y is the corresponding term for the interval 0.0 to 0.2. Data collected by ECOR method during 2004 to 2007 are used.

- *Light Use Efficiency (LUE)* is 19.4% and 203% larger for patchy clouds, and thick clouds than those for clear skies while *LUE* is about -6% for aerosols or thin clouds than those for clear skies.
- *Evaporative Fraction (EF)* is 15.4%, 17.9% and 23.2% larger for aerosols or thin clouds, patchy clouds, and thick clouds than those for the clear sky

Wang, K, R. E. Dickinson, and S. Liang (2008). Observational evidence on the effects of clouds and aerosols on net ecosystem exchange and evapotranspiration. *Geophysical Research Letter*, 35, doi:10.1029/2008GL034167



UNIVERSITY OF
MARYLAND



Black et al. 2006

Fig. 7. Relationship between apparent light use efficiency (ϵ_g)^{*} and the diffuse fraction of irradiance ($R_d:R_s$) for the grassland, barley and forest canopies. Data were used between April and August 2003, when the air temperature ranged between 5 and 10 °C. All linear relationships were significant at $P < 0.05$. ^{*} ϵ_g is based on absorbed irradiance by the canopy, but this does not account for the effect of diffuse fraction on light absorption (see Section 2).



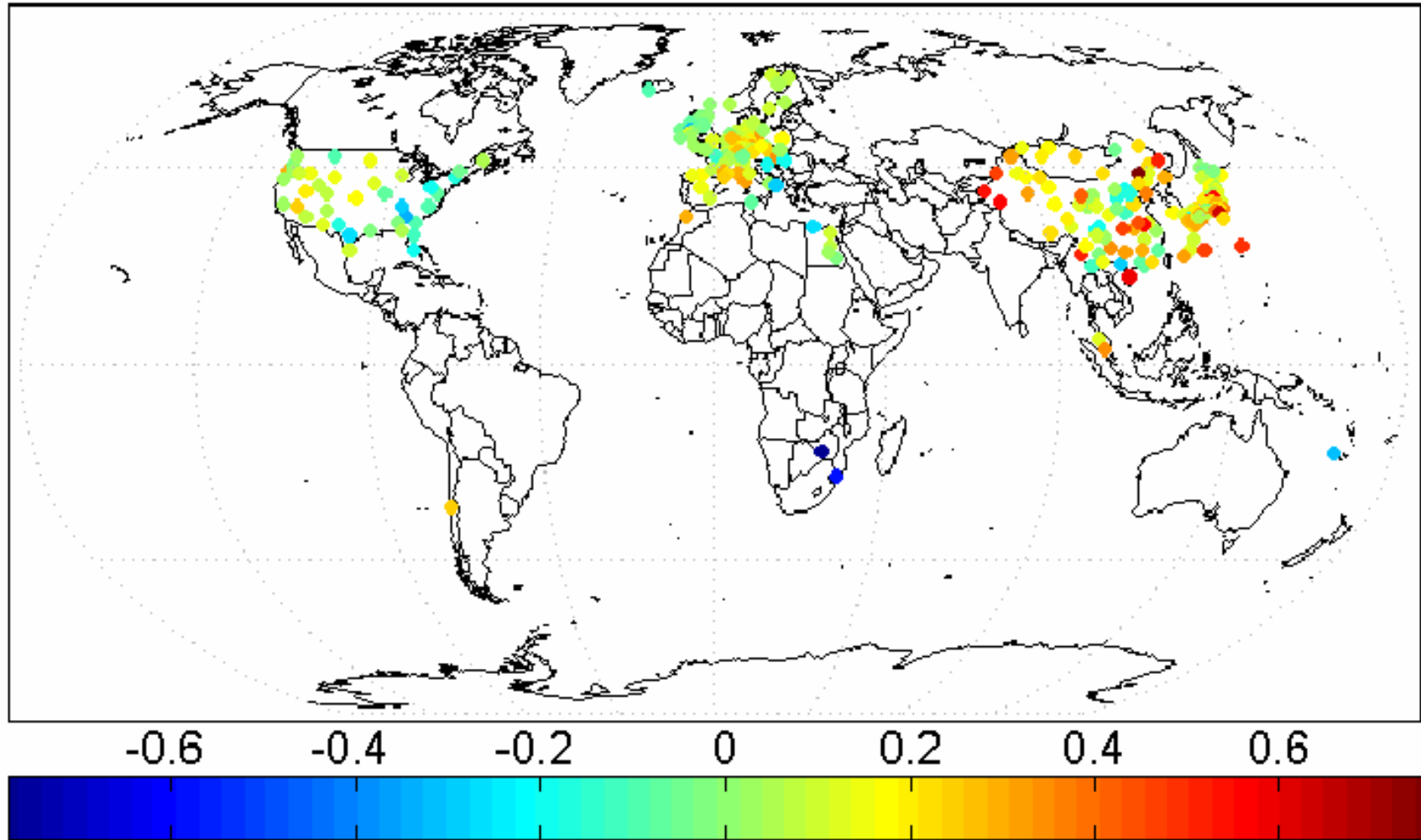
Long-term ET trend

Liang, et al.

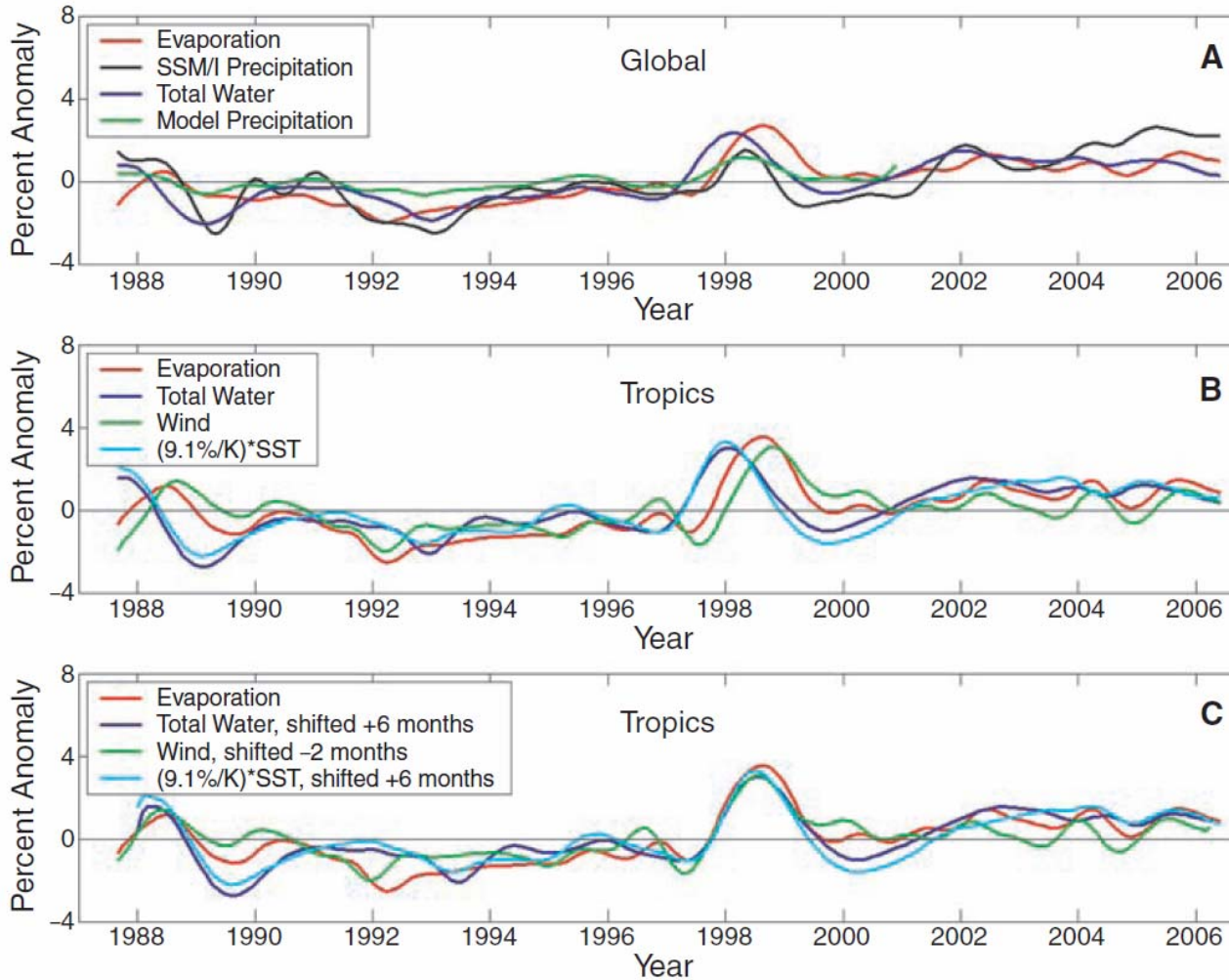
- ♣ Terrestrial evaporation cools and moistens the atmosphere near the earth's surface. The question of whether long-term global terrestrial evaporation is increasing, decreasing or constant remains controversial.
- ♣ We developed a new algorithm to estimate land surface evapotranspiration from remote sensing and other data
 - Wang, K., S. Liang, (2008), An improved method for estimating global evapotranspiration based on satellite determination of surface net radiation, vegetation index, temperature, and soil moisture, *Journal of Hydrometeorology*, 9(4):712-727.
- ♣ We found an average (over 265 sites) increase in terrestrial evaporation of $0.112 \text{ W m}^{-2} \text{ yr}^{-1}$, or 2.25 W m^{-2} (6% in relative value) over the 21 years, equal to 28 mm yr^{-1} in water flux.
 - Wang, K., M. Wild, R. E. Dickinson, and S. Liang, (2008), Increase in global terrestrial evaporation from 1982 to 2002. *Journal of Geophysical Research*



UNIVERSITY OF
MARYLAND



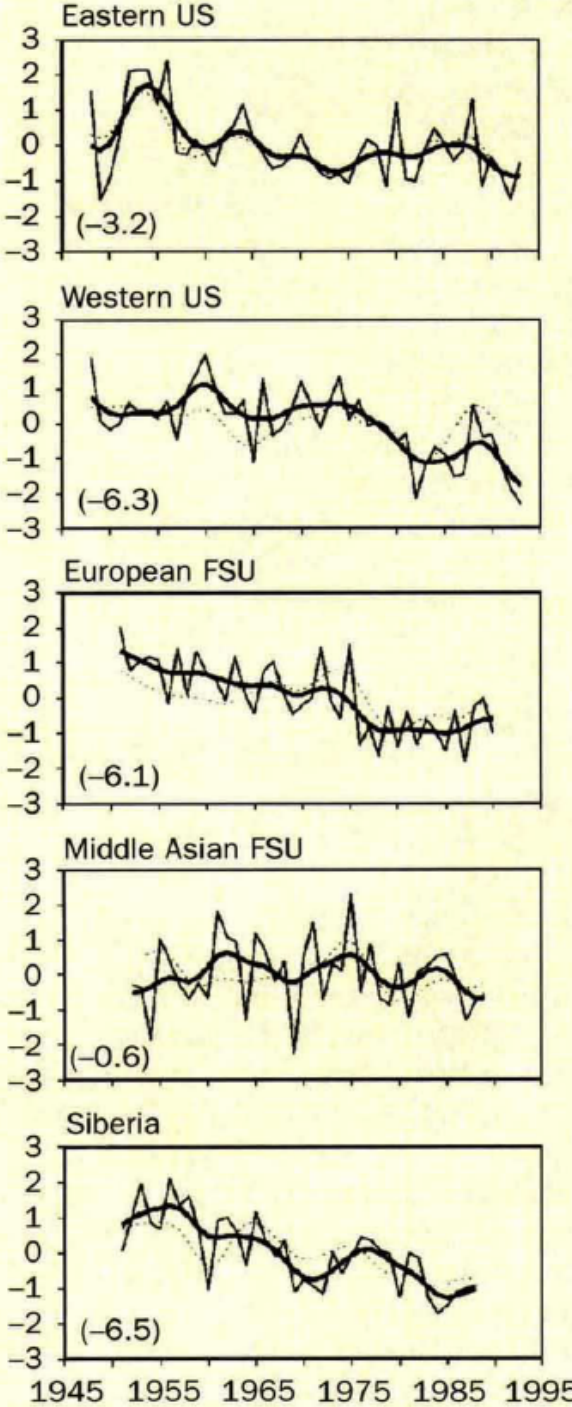
The trend in global terrestrial annual ET in units of $W\ m^{-2}\ yr^{-1}$ from 1982 to 2002. ET increases at 77% of the 265 stations shown. The average change in ET for all stations is $0.112\ W\ m^{-2}\ yr^{-1}$ and is $2.25\ W\ m^{-2}$ (28 mm) for the last 20-year period, equal to 6% of their average value.



Wentz et al.,
2007

Fig. 2. Anomaly time series of the hydrologic variables. **(A)** Global results for the observed precipitation and evaporation and over-ocean results for total water vapor. The average model precipitation predicted by AMIP simulations is also shown. **(B)** Tropical ocean results for evaporation, total water vapor, surface-wind speed, and SST. The SST time series has been scaled by $9.1\% \text{ K}^{-1}$. During the El Niños, evaporation and wind were not in phase with vapor and SST. At the end of 1996, SST and vapor began to increase while the winds began to decrease, with no net effect on evaporation. About 8 months later (mid-1997), the winds in the tropics began to recover and then increased sharply, reaching a maximum value in late 1998. All four variables remained at elevated values thereafter. **(C)** Same as **(B)**, except that the water vapor and SST curves have been shifted forward in time by 6 months, and the wind curve has been shifted backward by 2 months. The statistics on the global time series, including error bars, are given in Table 1.

Standardized anomaly



Area-average pan evaporation (solid lines) and diurnal temperature range (DTR, dotted line, updated from Karl et al.¹) for three regions in the former Soviet Union and two regions in the United States. All time series are presented as standard deviation anomalies from the long-term mean values. The smooth curves result from 11-point binomial smoothing (for DTR only smoothed lines are presented). Linear trend estimates for these regions (in standardized anomalies per 100 yr) are shown in parentheses. They are significant at the 99% level except for the former Soviet Union Middle Asian region. The largest actual change in pan evaporation is in the western United States, where the area-averaged linear regression slope corresponds to a decrease in pan evaporation of 97 mm per warm season (May–September) during the past 45 years in a region with a mean pan evaporation of 1,130 mm per warm season.



Current solar radiation products

Liang, et al.

- ♣ The ISCCP (International Satellite Cloud Climatology Project) solar radiation products at 280 km (1983-2000);
- ♣ The Global Energy and Water Cycle Experiment (GEWEX) SRB Release 2 has a spatial resolution of $1^\circ \times 1^\circ$;
- ♣ The Clouds and the Earth's Radiant Energy System (CERES) flux products at 140km;
- ♣ GCM reanalysis products ($> 1^\circ$)

Table 2. Downward Solar Radiation at the Surface and Absorbed Solar Radiation at the TOA Observed at 760 GEBA Sites and Calculated by the 20 GCMs Participating in AMIPII^a (Wild, et al., 2005)

	Model Mean	Observed	Mean Bias	Range of Biases	St. Dev. Biases	Mean Corr.
SW down surface	178	169	+9	-9 to 31	10	0.91
SW absorbed TOA	219	218	+1	-10 to 8	6	0.96

^aLong-term annual mean averages over all sites: multimodel-mean, observed, mean model bias, range of individual model biases, standard deviation of model biases, multimodel-mean correlations. Surface observations from GEBA, TOA observations collocated with GEBA sites from ERBE. Units Wm^{-2} , except for correlation coefficients.



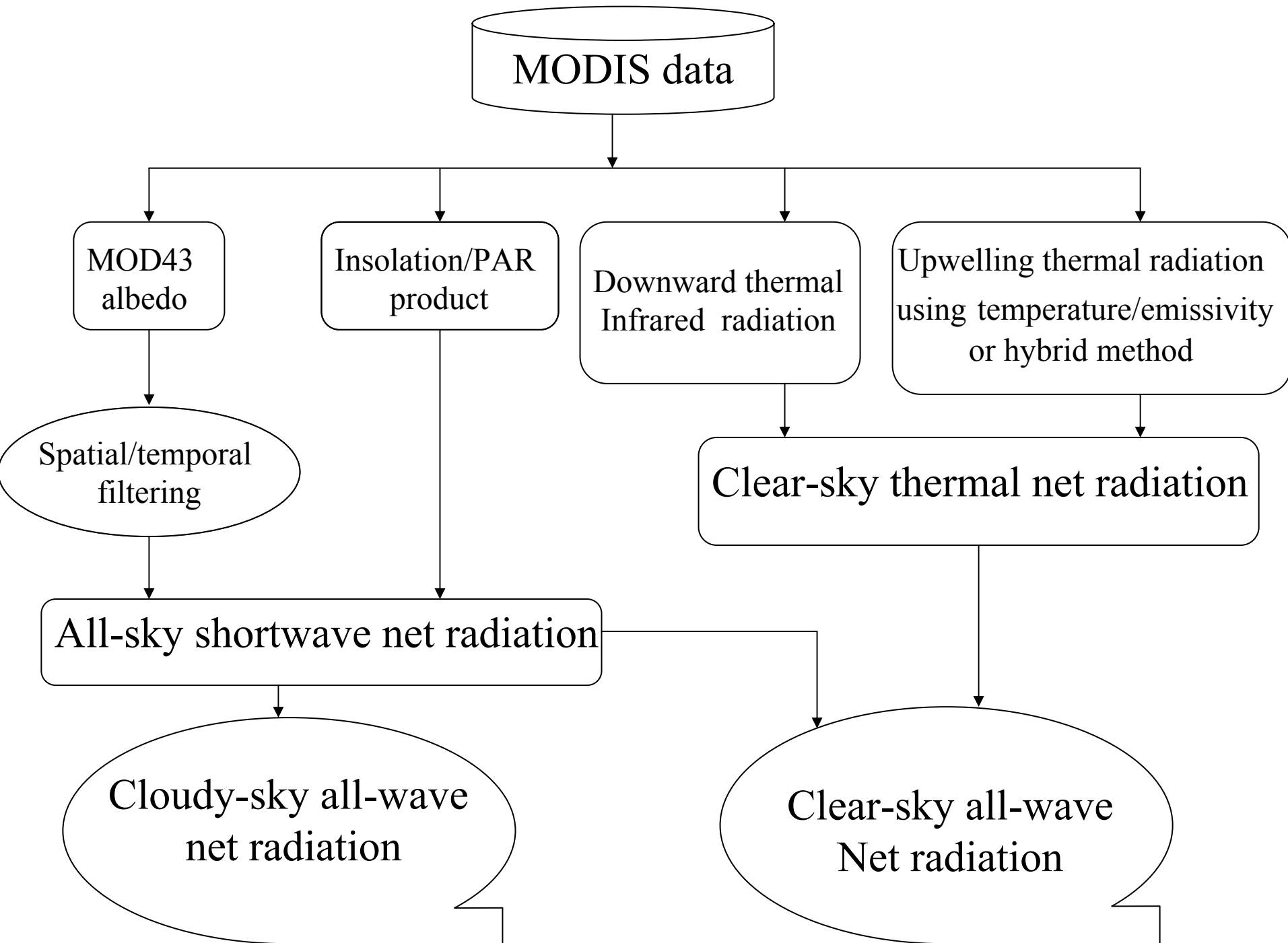
Need for high spatial resolution products

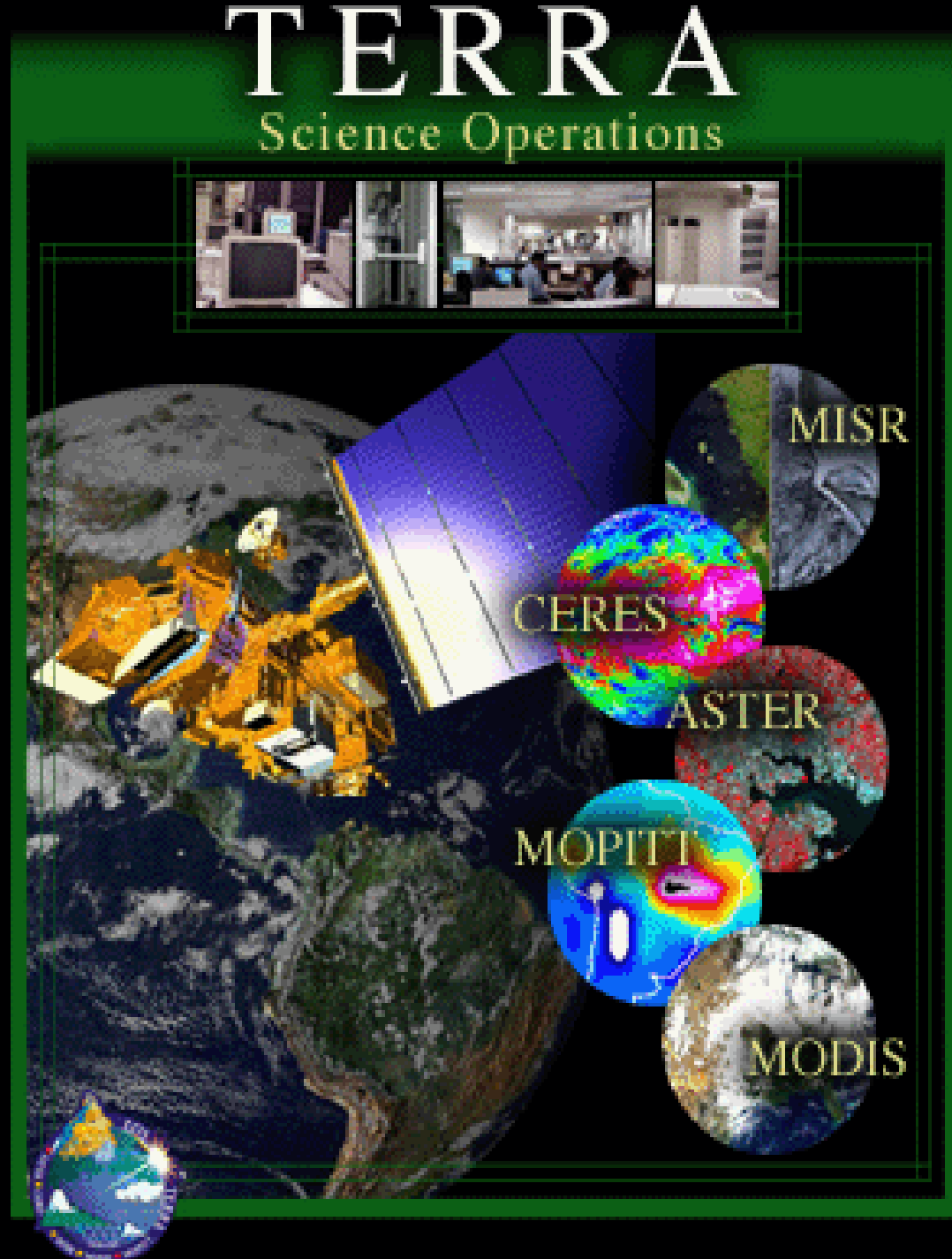
Liang, et al.

- ♣ Current global radiation products have coarse spatial resolution ($>1^\circ$) but fine temporal resolution (3 hours), primarily for atmospheric modeling
- ♣ Those products do not account for many local features, such as urbanization.
- ♣ Land applications require high spatial resolution (~1km) but reasonable temporal resolution (e.g., daily)
 - Ecosystem modeling (say, MODIS NPP product) requires high-resolution products (1km)
 - Hydrological modeling (ET) at 1km
 - Other applications on environmental monitoring (e.g., drought detection)



UNIVERSITY OF
MARYLAND







Estimation of insolation/PAR

Liang, et al.

Liang, S., T. Zheng, R. Liu, H. Fang, S. C. Tsay, S. Running, (2006), Estimation of incident Photosynthetically Active Radiation from MODIS Data, *Journal of Geophysical Research –Atmosphere*. 111, D15208, doi:10.1029/2005JD006730.

Liu, R., S. Liang, H. He, J. Liu, and T. Zheng, (2008), Mapping Photosynthetically Active Radiation from MODIS Data in China. *Remote Sen. Environ.* 112:998-1009



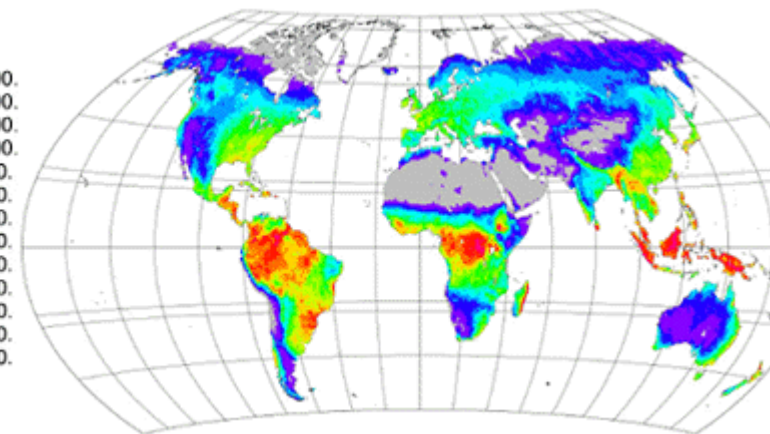
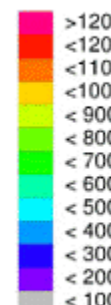
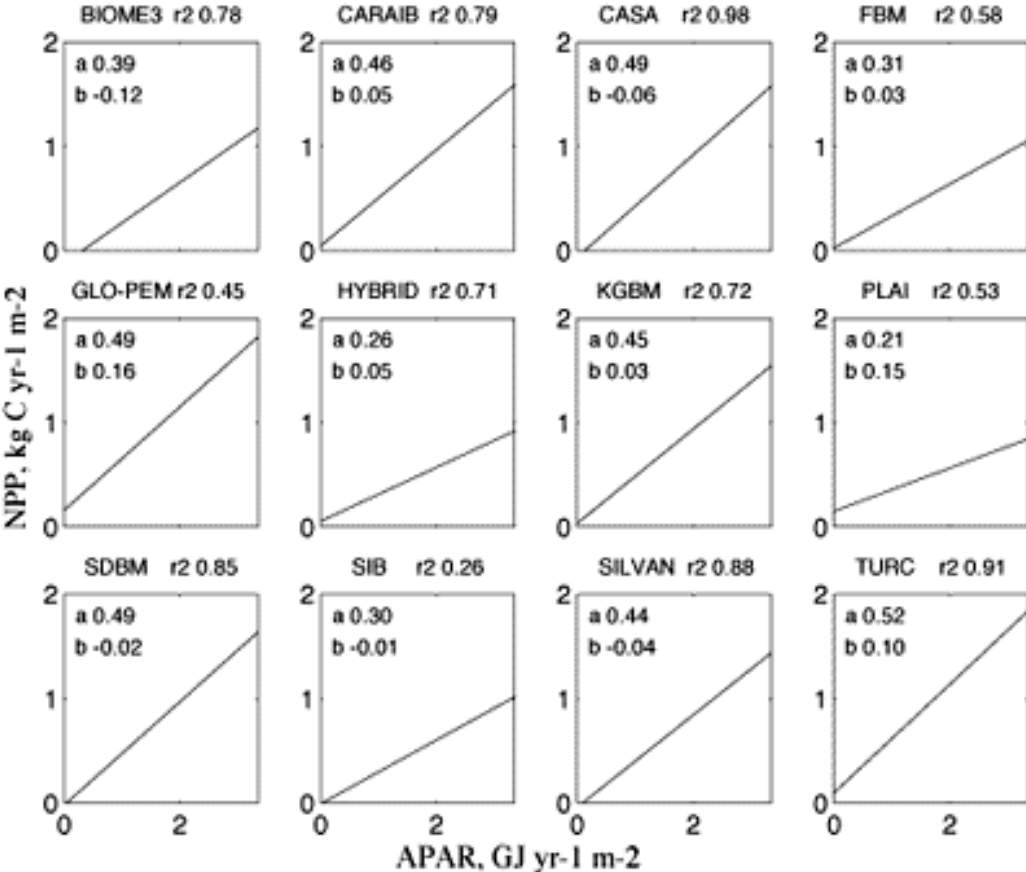
Liang, et al.

Production Efficiency Principles:

$$GPP = \varepsilon_g \bullet fPAR \bullet PAR$$

$$NPP = \varepsilon_n \bullet fPAR \bullet PAR$$

where PAR (MJ m⁻²) is in a time period (day, month), FAPAR is the fraction of PAR absorbed by vegetation canopy, and ε_g is the light use efficiency (LUE, g C MJ⁻¹ PAR) in GPP calculation, and ε_n is the light use efficiency in NPP calculation.

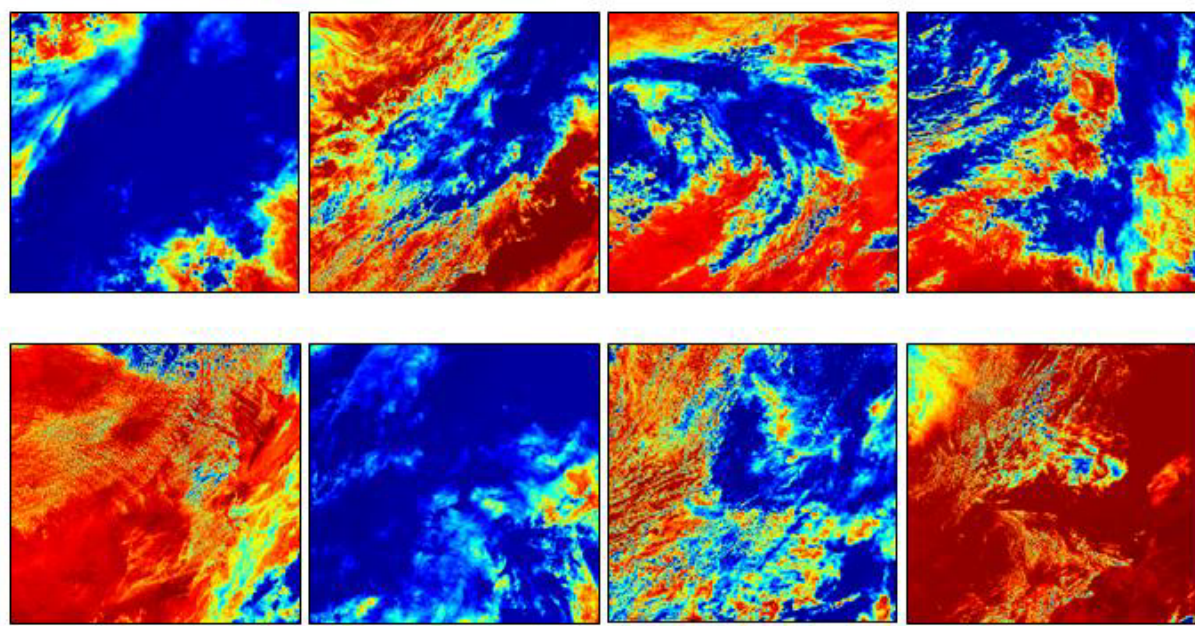


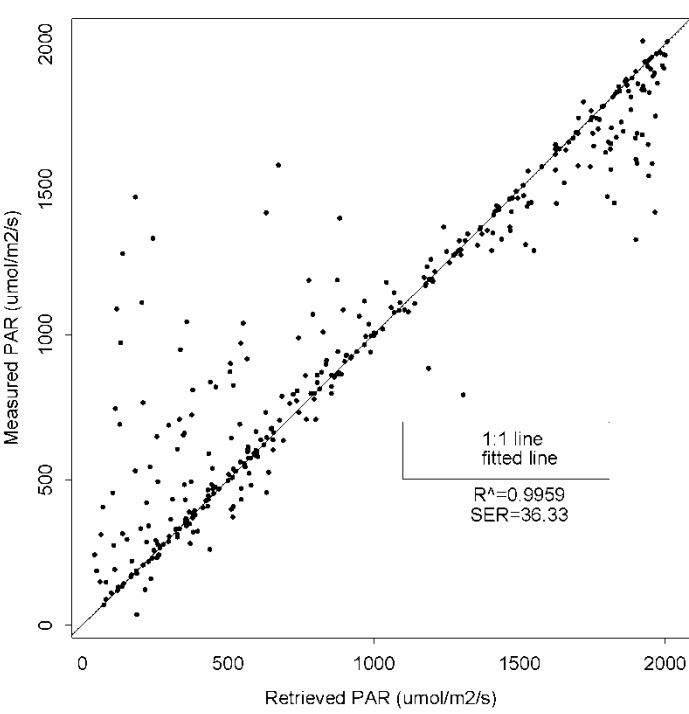
Annual net primary production (g C m⁻² yr⁻¹) estimated as the average of all model NPP estimates.

Grid cell level regression of net primary production (NPP) (kg C yr⁻¹ m⁻²) against absorbed photosynthetically active radiation (APAR) (GJ yr⁻¹ m⁻²)

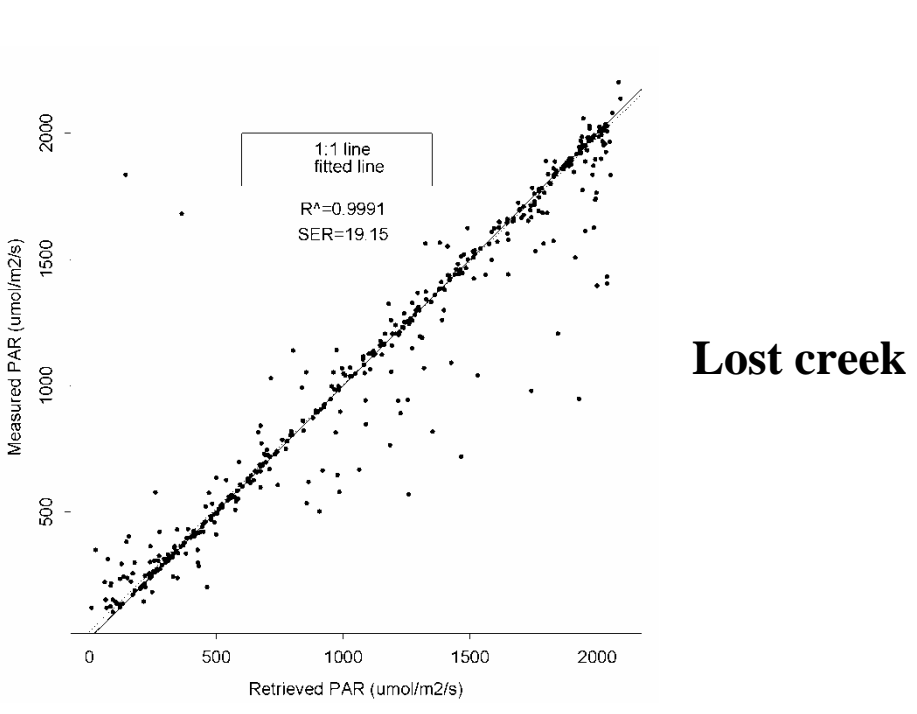
Cramer, et al., 1995, Net primary productivity model inter-comparison activity, IGBP/GAIM report series 5

MODIS TOA radiance on 8 days in 2003: May 22, May 25, May 29, May 31, June 5, June 7, June 8, and June 10

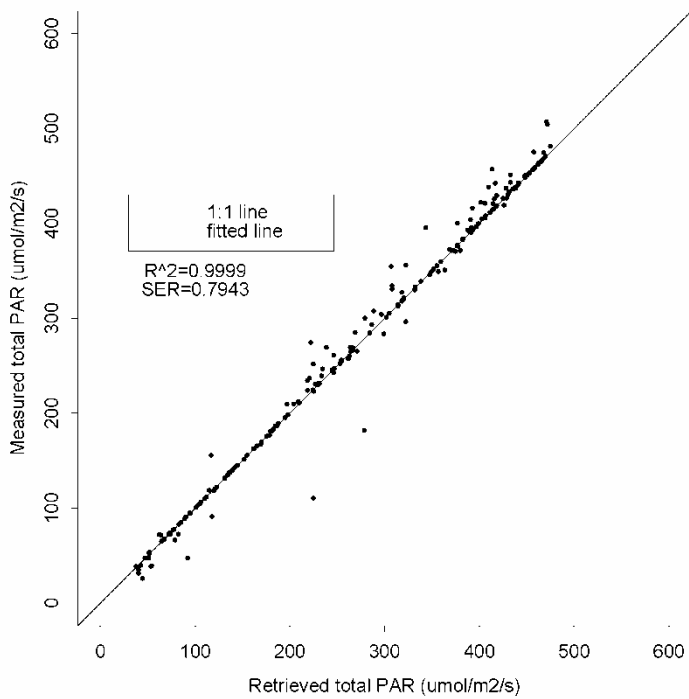




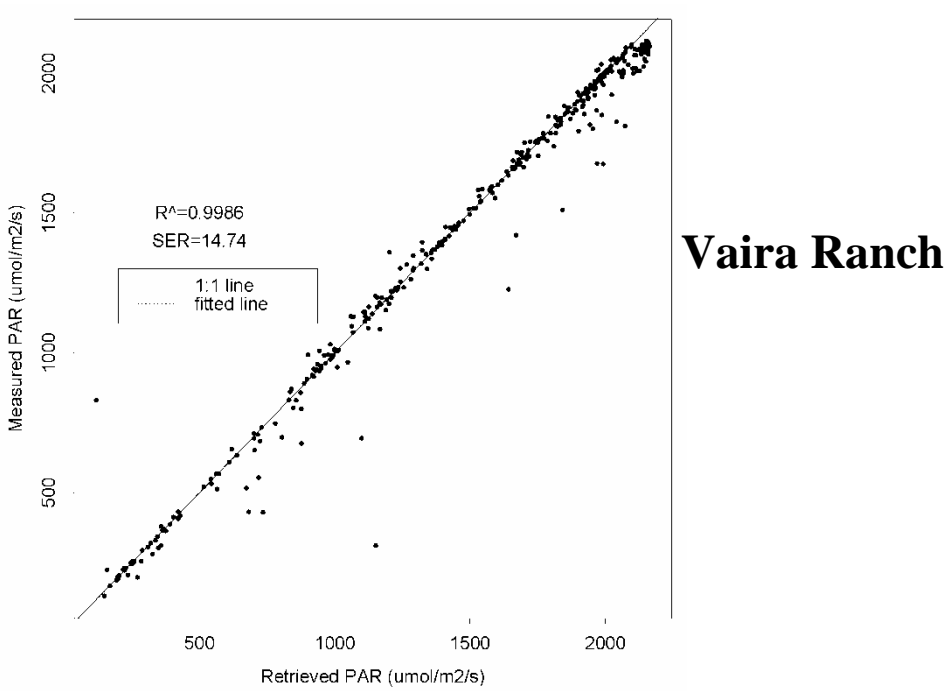
Fort Peck



Lost creek



Oak Ridge



Vaira Ranch



Liang, et al.

Temporal scaling (daily insolation/PAR)

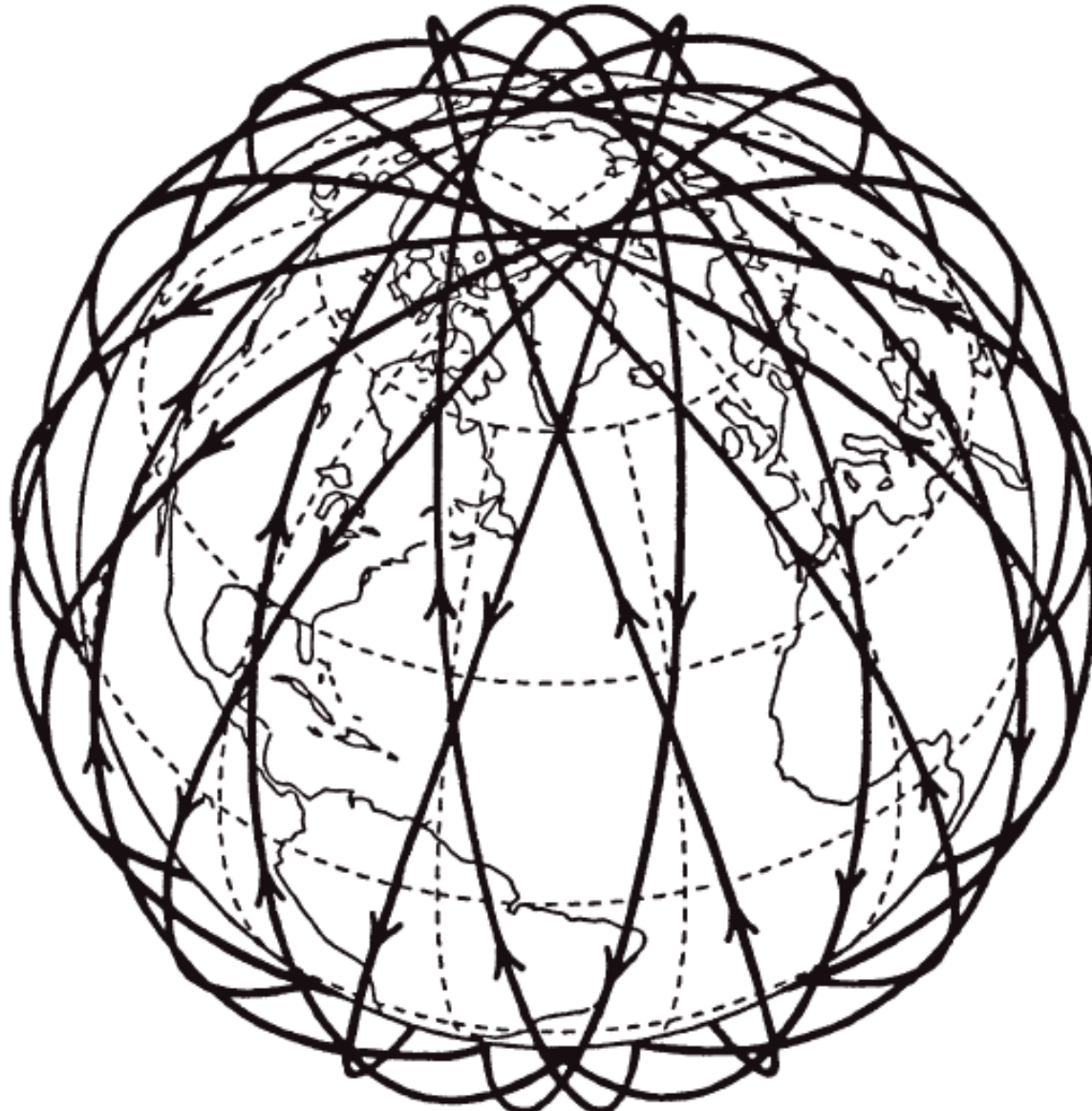
(1). Terra/Aqua MODIS alone;

* Wang, D., Liang, S. and Zheng, T., Integrated daily PAR from MODIS. *International Journal of Remote Sensing*, in press.

(2). Integration with geostationary (GOES) product

* Zheng, T., S. Liang & D. Wang, (2008), Estimation of incident PAR from GOES imagery, *Journal of Applied Meteorology and Climatology*. 47:853-868 .

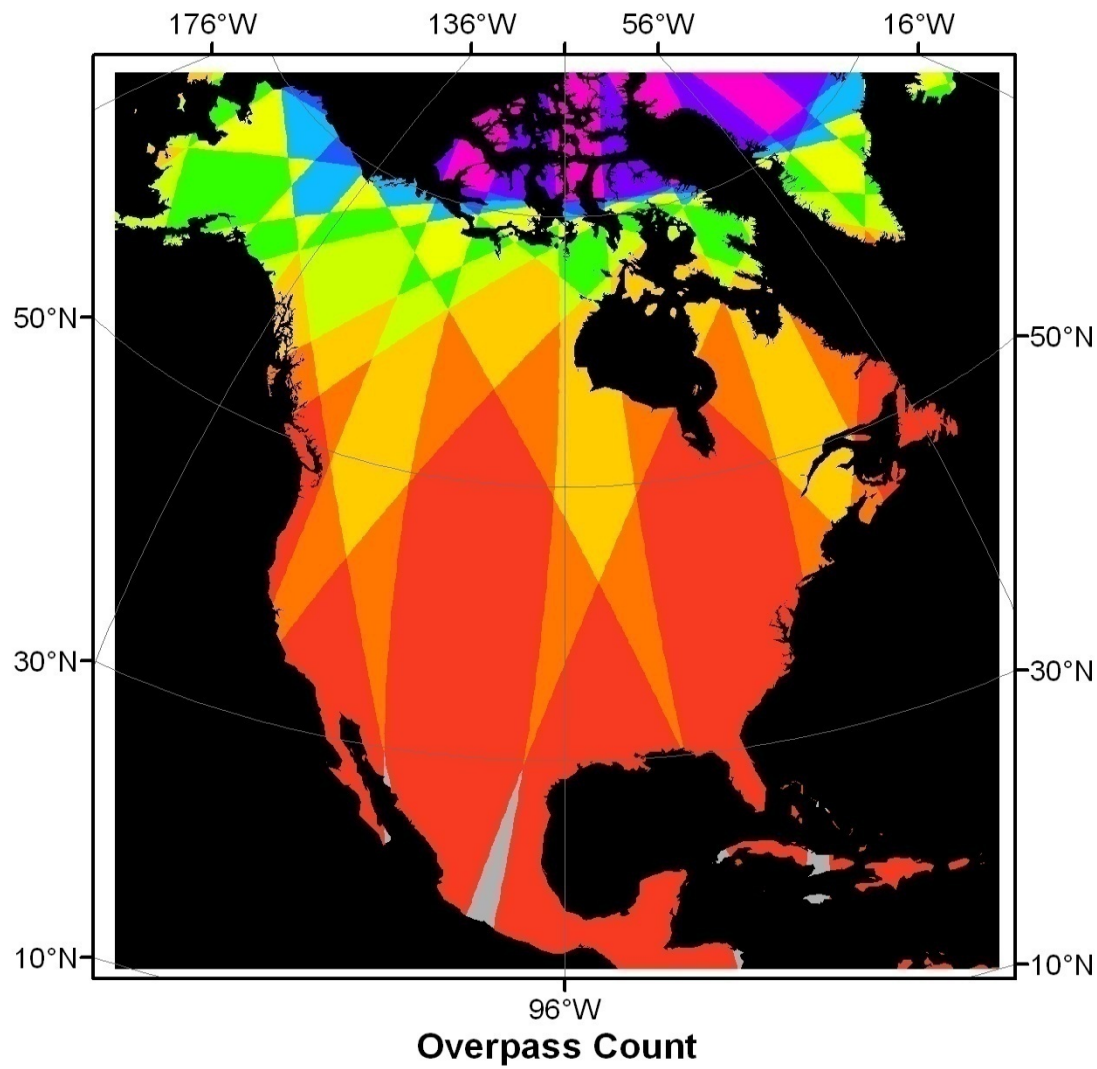
* Wang, K., S. Liang, T. Zheng, and D. Wang, Simultaneous estimation of surface photosynthetically active radiation and albedo from GOES, *Remote Sensing of Environment*. revised.



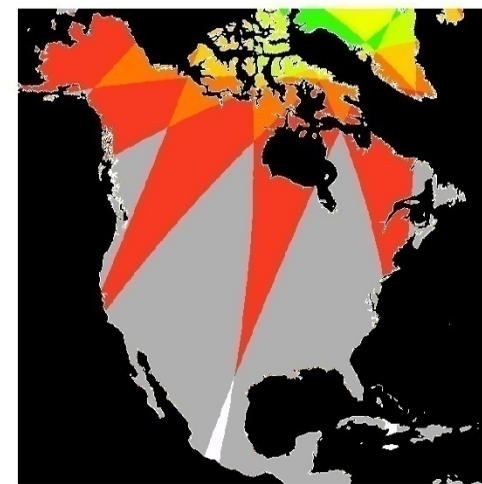
One day's orbits of a sun-synchronous satellite. A single instrument views the entire Earth. SOURCE: Kidder and Vonder Haar (1995). Copyright Elsevier, 1995.

Daytime MODIS Overpass Over North America

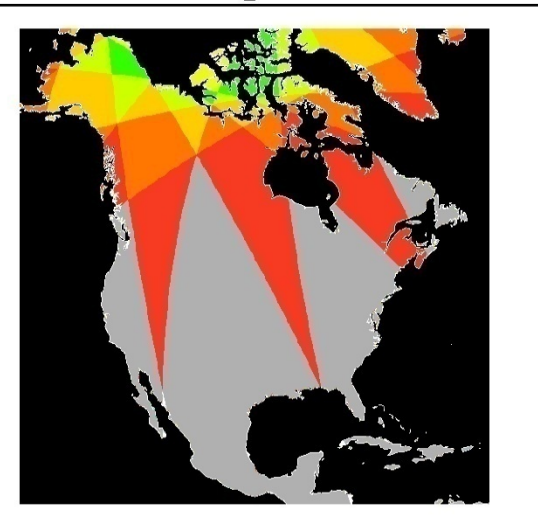
Both Terra and Aqua (June 16, 2006)



Terra

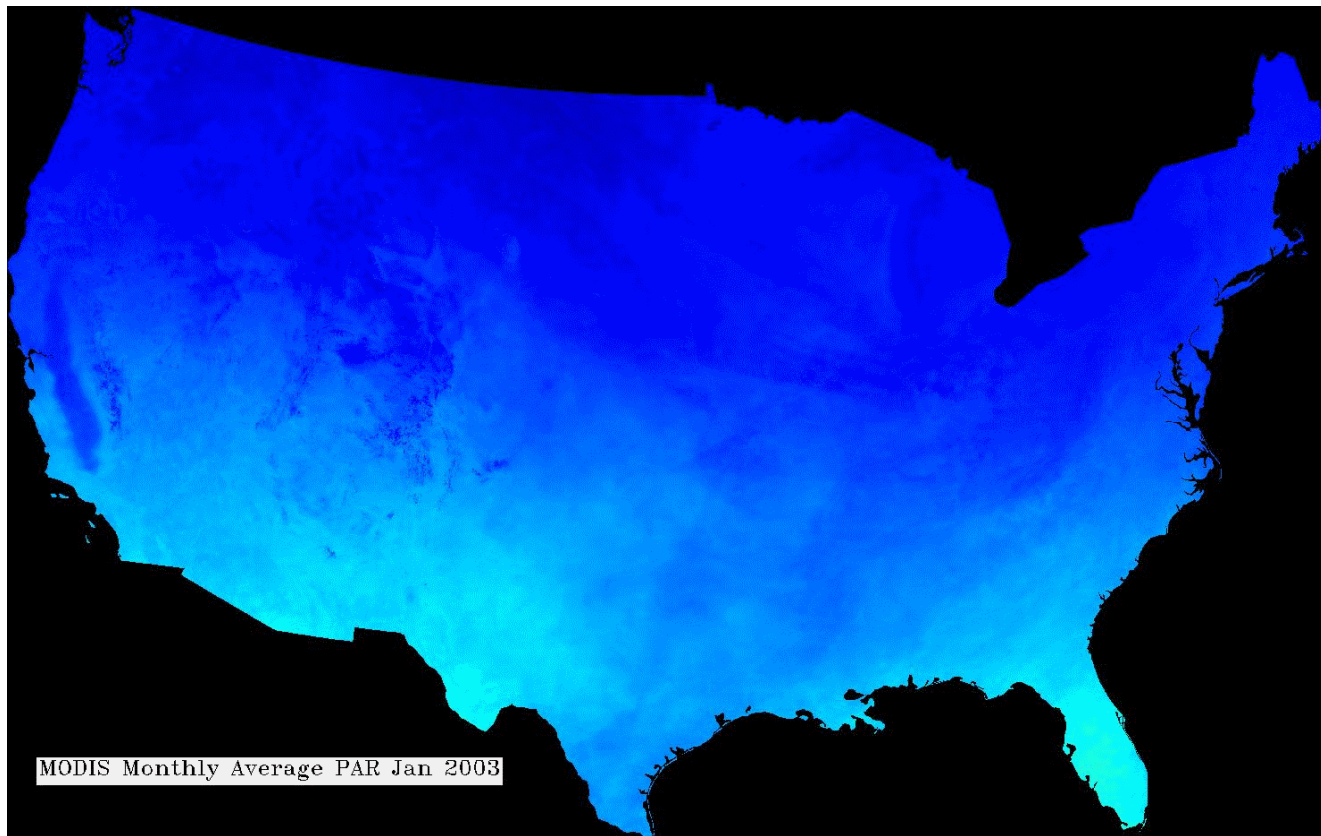


Aqua





Monthly PAR from MODIS



Liang, et al.

Three years (2003-2005) daily incident PAR at 4km over North America available now; Bob Cook has kindly agreed to distribute them at ORNL DAAC.



Spatial/temporal filtering

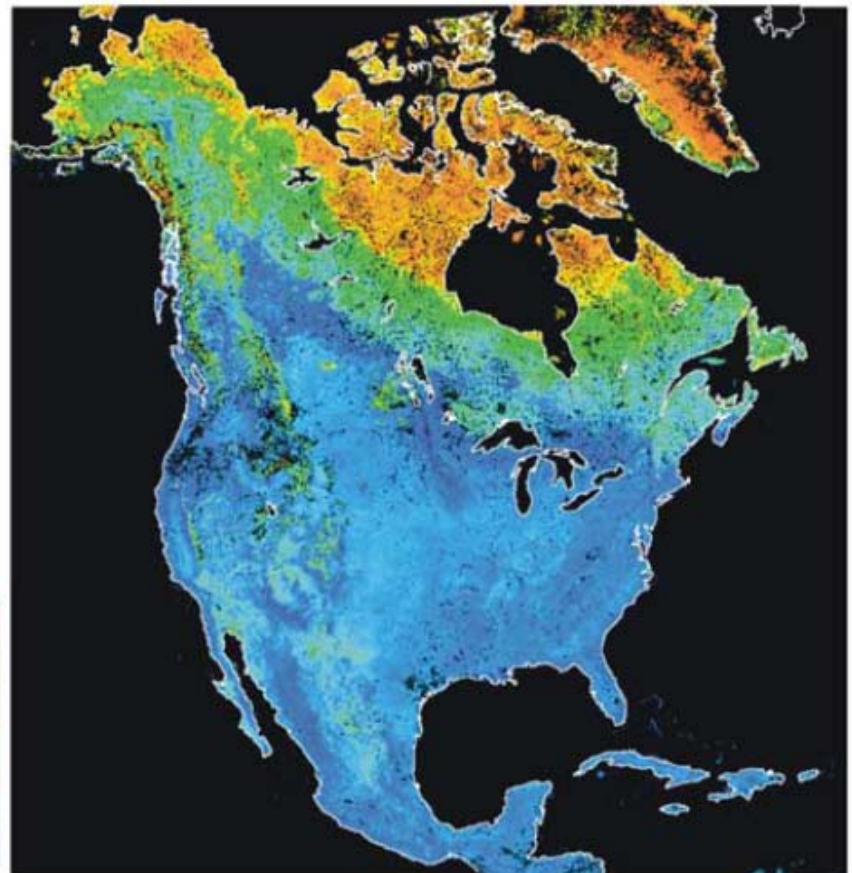
Liang, et al.

Fang, H., S. Liang, H. Kim, J. Townshend, C. Schaaf , A. Stralher, R. Dickinson, (2007), **Developing spatially continuous 1km surface albedo dataset over North America from Terra MODIS products**, *Journal of Geophysical Research*, 112, doi:10.1029/2006JD008377

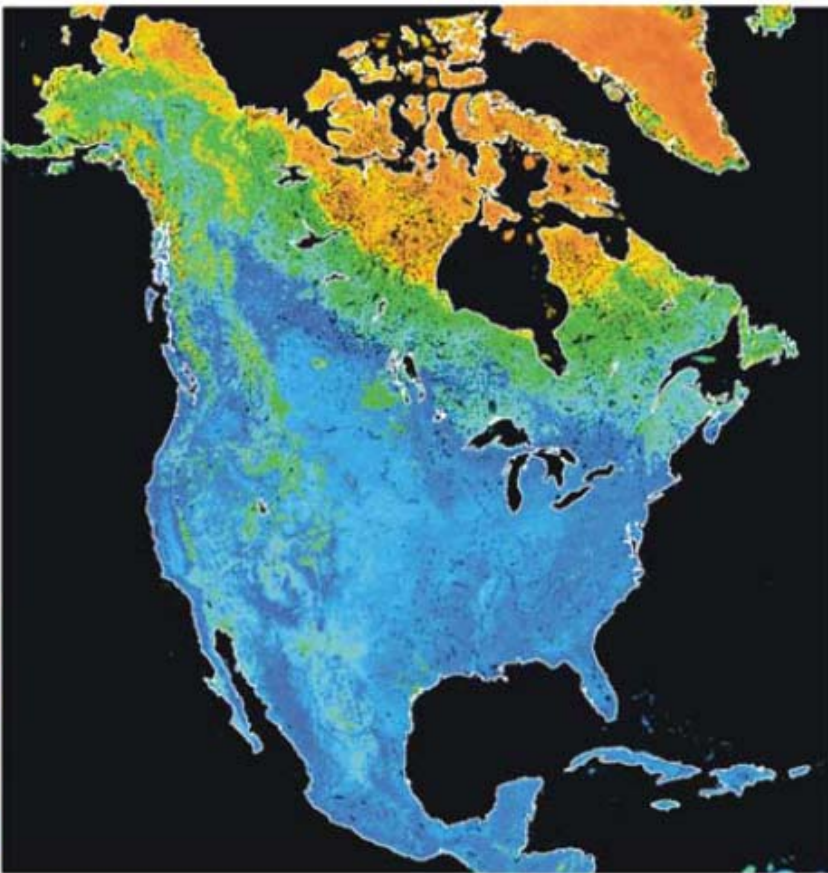


UNIVERSITY OF
MARYLAND

A



B



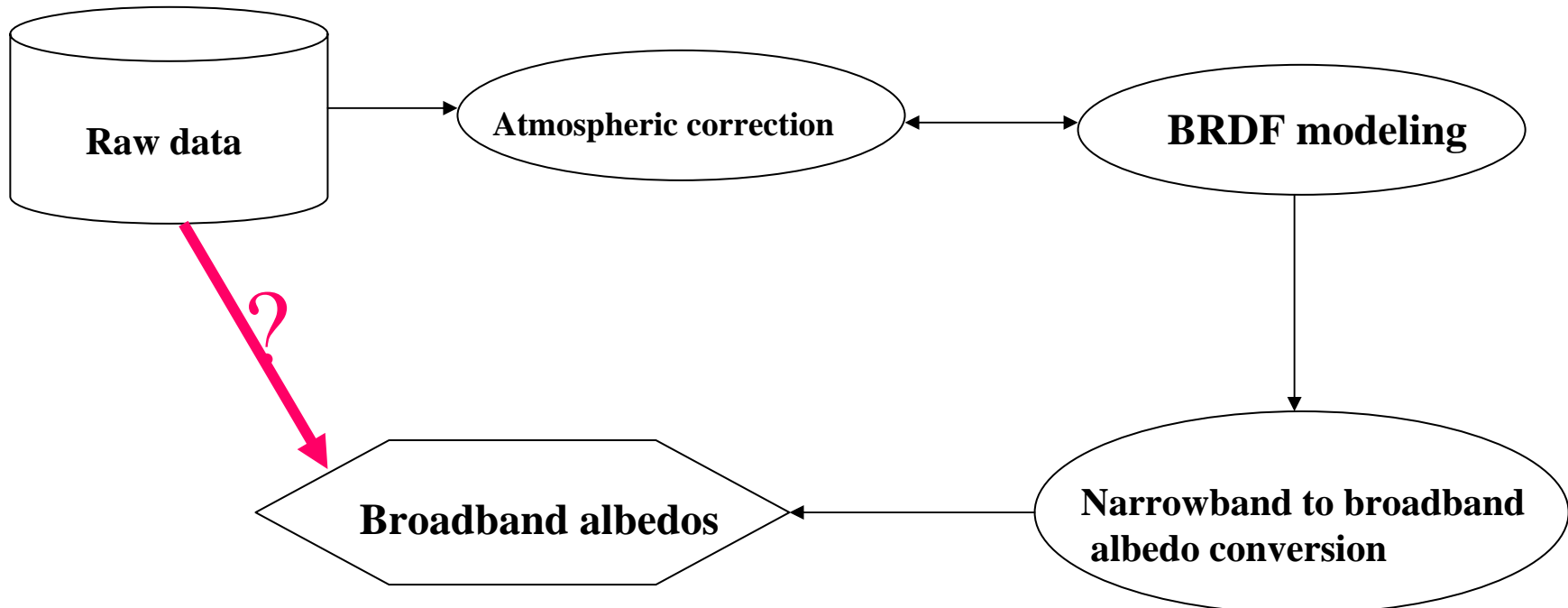
North America total shortwave black-sky albedo (DOY 97–112, 2001). (a) The original MODIS albedo; (b) Derived with the new filter

Fang, H., S. Liang, H.-Y. Kim, J. R. Townshend, C. L. Schaaf, A. H. Strahler, and R. E. Dickinson (2007), Developing a spatially continuous 1 km surface albedo data set over North America from Terra MODIS products, *J. Geophys. Res.*, 112, doi:10.1029/2006JD008377.



Broadband albedo estimation

Liang, et al.



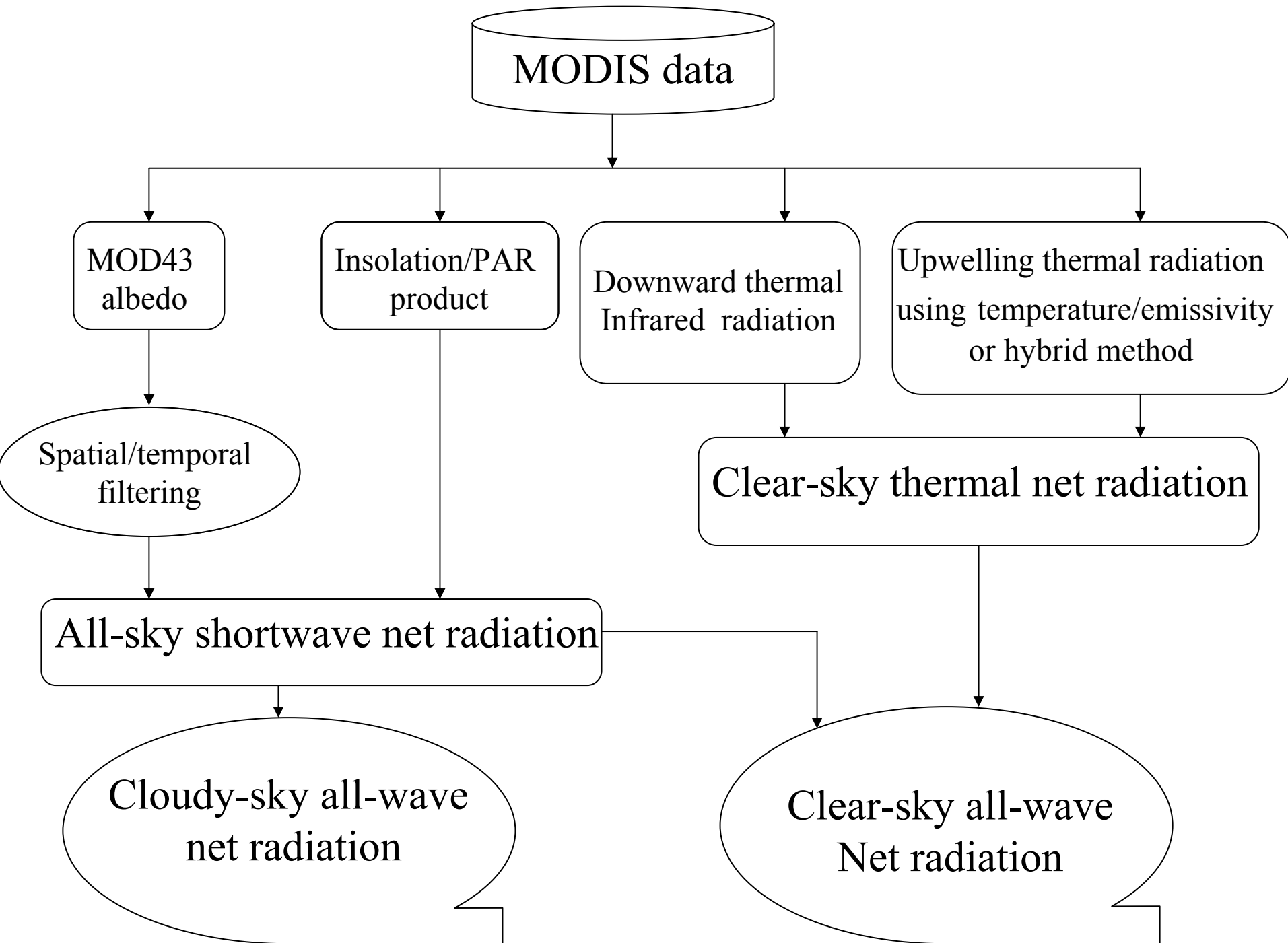
Liang, S., A direct algorithm for estimating land surface broadband albedos from MODIS imagery, *IEEE Trans. Geosci. Remote Sen.*, 41(1):136-145, 2003;

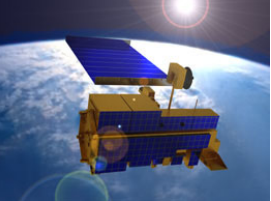
Liang, S., J. Stroeve and J. Box, (2005), *Mapping daily snow shortwave broadband albedo from MODIS: The improved direct estimation algorithm and validation*, *Journal of Geophysical Research*. 110 (D10): Art. No. D10109.



Liang, et al.

- ♣ This algorithm has been used as the default algorithm for the VIIRS (Visible/Infrared Imager/Radiometer Suite) in the NPOESS (National Polar-orbiting Operational Environmental Satellite System) and NPP (NPOESS Preparatory Project) program
- ♣ The similar idea is being applied to GOES-R albedo production generation





Estimation of downward thermal radiation

Liang, et al.

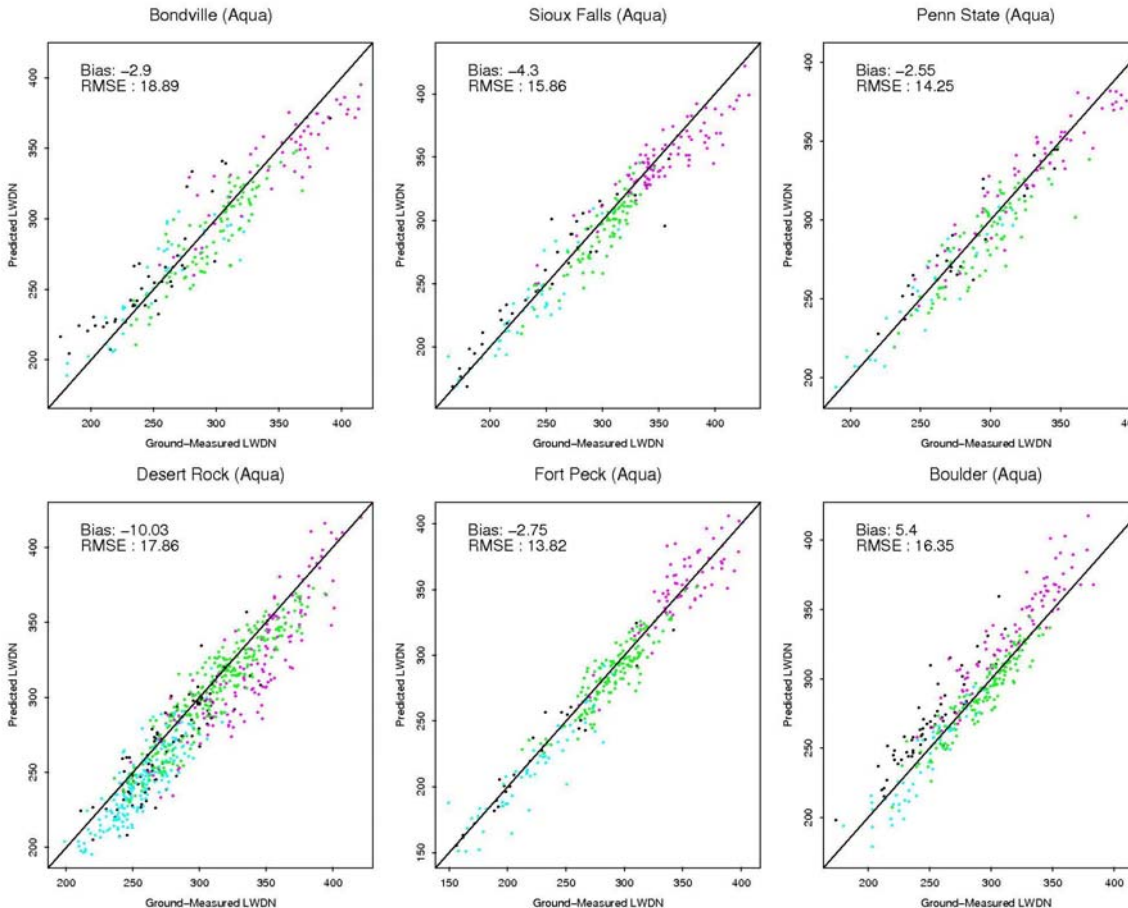
- 1). Calculating downward flux using atmospheric profiles
- 2). Calculating downward flux from TOA radiance directly

Wang, W. & S. Liang, Estimating High-Spatial Resolution Clear-Sky Land Surface Downwelling and Net Longwave Radiation from MODIS Data, *Remote Sensing of Environment*, in press



Estimating LWDN: Validation (Aqua)

Liang, et al.



- ♣ Results similar to Terra
- ♣ Smaller RMSEs in Aqua-derived LWDN
 - Smaller systematic errors in Aqua (Liu et. Al, 2006)
 - Diff. overpass times
→ diff. atmospheric conditions

Avg. RMSE: 17.60 W/m²
Avg. Bias: -0.40 W/m²

Nonlinear Models

day/fallwinter
night/fallwinter
day/springsummer
night/springsummer



Estimating LWUP

(1) Temperature-Emissivity Method

Liang, et al.

$$F_u = \varepsilon \int_{\lambda_1}^{\lambda_2} \pi B(T_s) d\lambda + (1 - \varepsilon) F_d$$

T_s MODIS LST (MOD11_L2)

ε Broadband emis (derived from MOD11B1)

(2) Hybrid Method

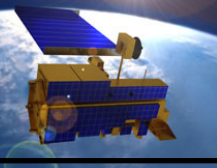
- ♣ Following the framework for hybrid methods
 - Emissivity Effect
 - UCSB Emissivity Library (59 spectra)
 - ~2000 MODIS Profile
- ♣ Statistical Analysis
 - Linear SULR Models ($R^2: 0.990$, $RMSE < 5.42 \text{ W/m}^2$)

$$F_u = a_0 + a_1 L_{29} + a_2 L_{31} + a_3 L_{32}$$

- Artificial Neural Network (ANN) Models ($R^2: 0.996$ $RMSEs < 3.7 \text{ W/m}^2$)

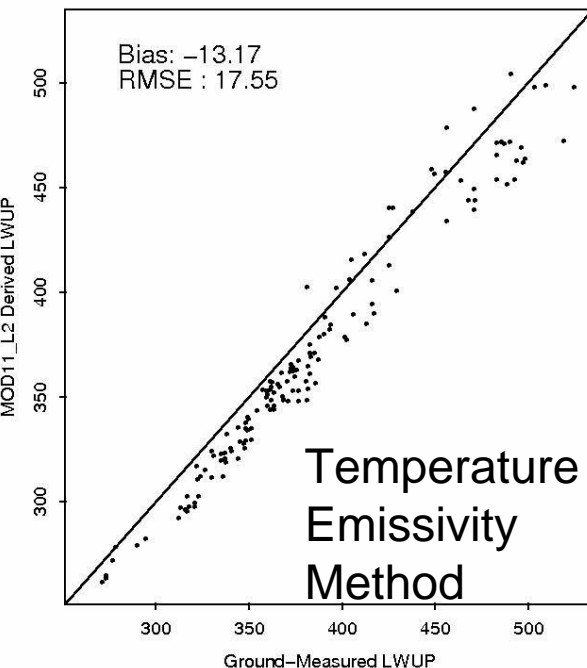
5 Models in total

θ	Model
0°	
15°	
30°	
45°	
60°	

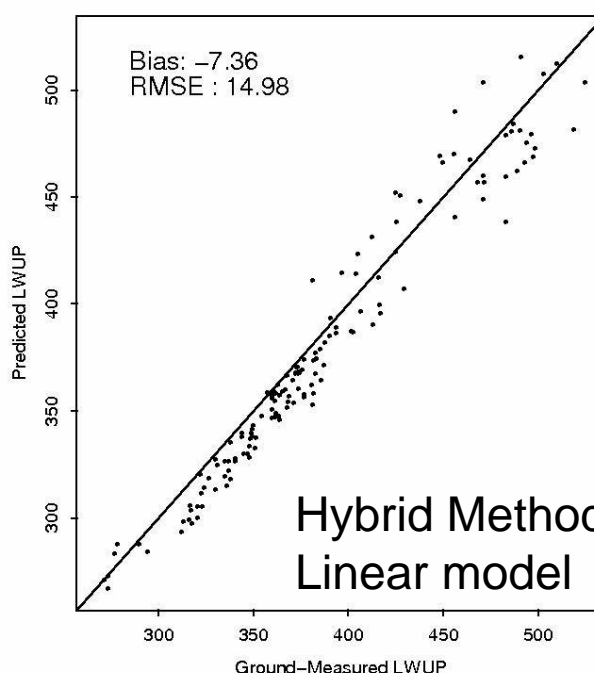


Estimating LWUP: validation

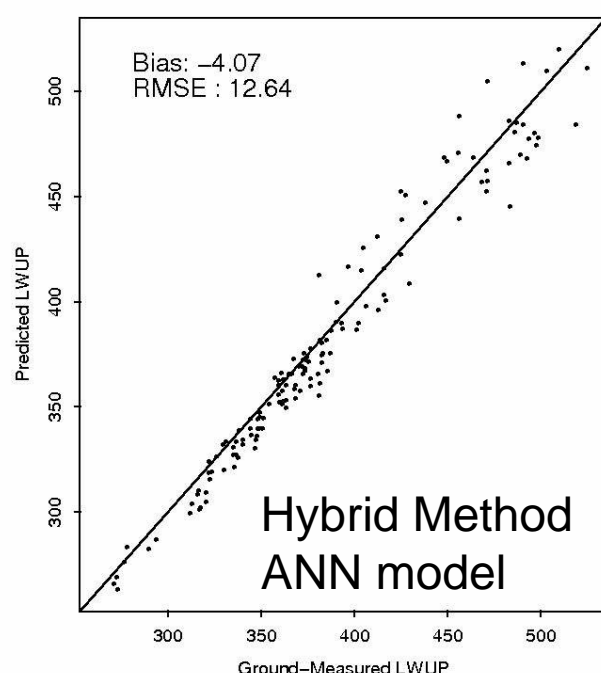
Bondville, IL (Aqua)



Bondville, IL (Aqua)



Bondville, IL (Aqua)



Bondville, IL (cropland, elevation 213 m)

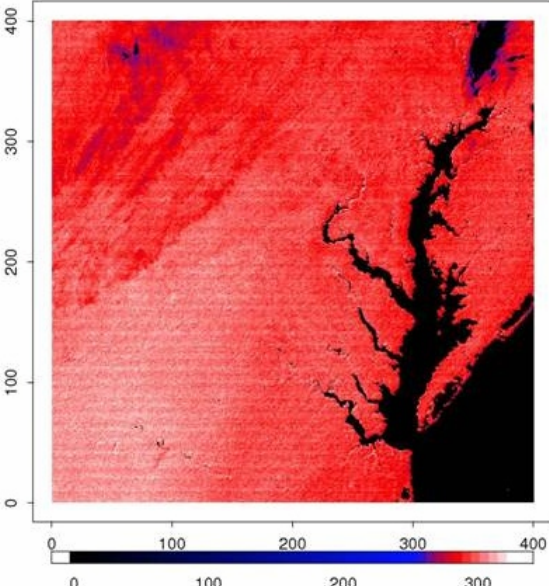
- Smaller RMSEs in Aqua
- Hybrid method outperforms temperature-emissivity method
- ANN model outperforms linear model

Wang, W., S. Liang & J. A. Augustine, (2008), Estimating Clear-Sky Land Surface Upwelling Longwave Radiation from MODIS Data. *IEEE Trans. Geosci. and Remote Sens.* 47(12)

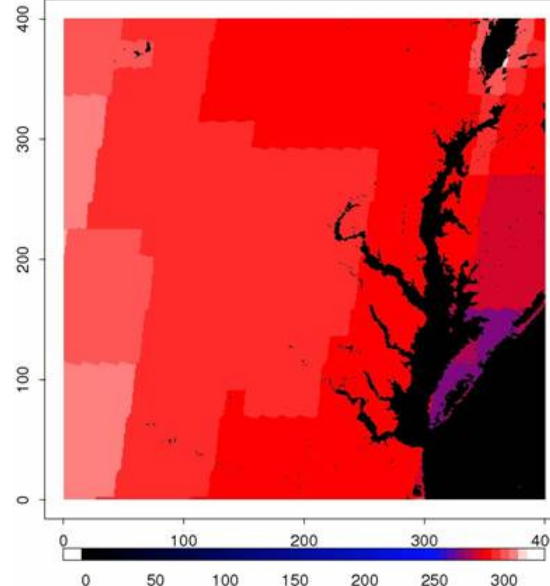
SURFRAD 6 sites	Temperature- Emissivity Method	Hybrid Method	
		Linear model	ANN model
Avg. RMSE	20.58	17.63	15.23
Avg. Bias	-17.25	-10.46	-7.94
Input Parameters	Surface temp. Emissivity, LWDN	TOA radiance	TOA radiance

- **Hybrid method: simple but smaller RMSEs**
- Sources of Error
 - Spatial mismatch
 - LWUP sensitive to surface conditions
vegetation cover, snow, soil moisture ...
 - Sensor error
 - Cloud contamination ([Wang et al, 2007; Wan, 2008](#))
- Systematic Bias
 - Systematic error in MODIS channels
 - Cloud contamination →
lower retrieved surface temp., emissivity and LWUP

LWDN (MODIS)



LWDN (CERES)



LWDN

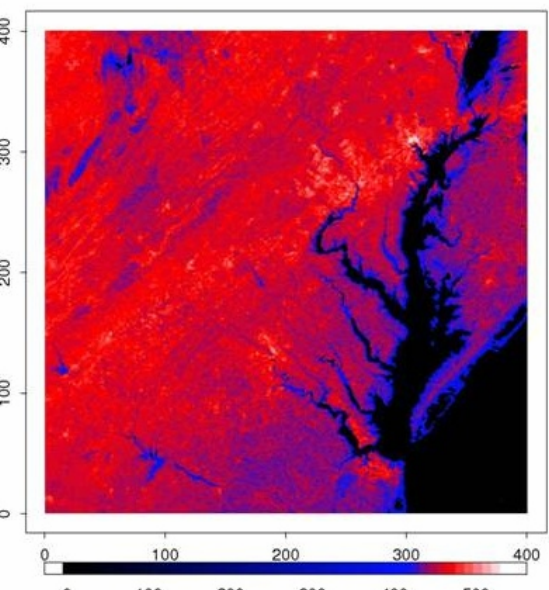
- Avg. Diff. : ~5 W/m²

CERES:

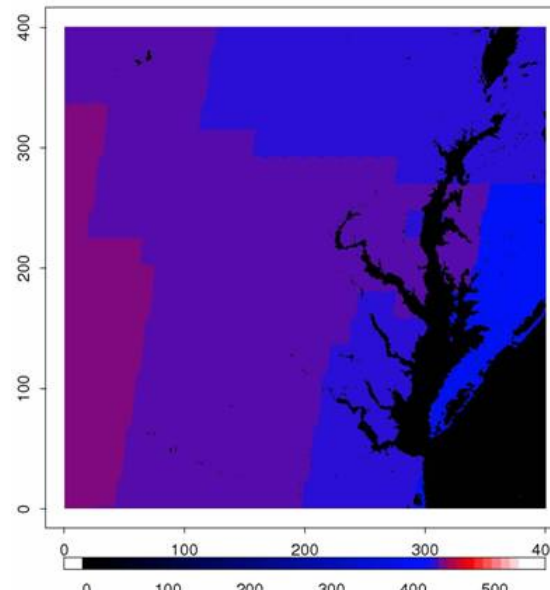
highly parameterized
equations (*Gupta et al., 1997*)

- MODIS: hybrid method

LWUP (MODIS)



LWUP (CERES)



LWUP

- Avg. Diff. : ~27 W/m²

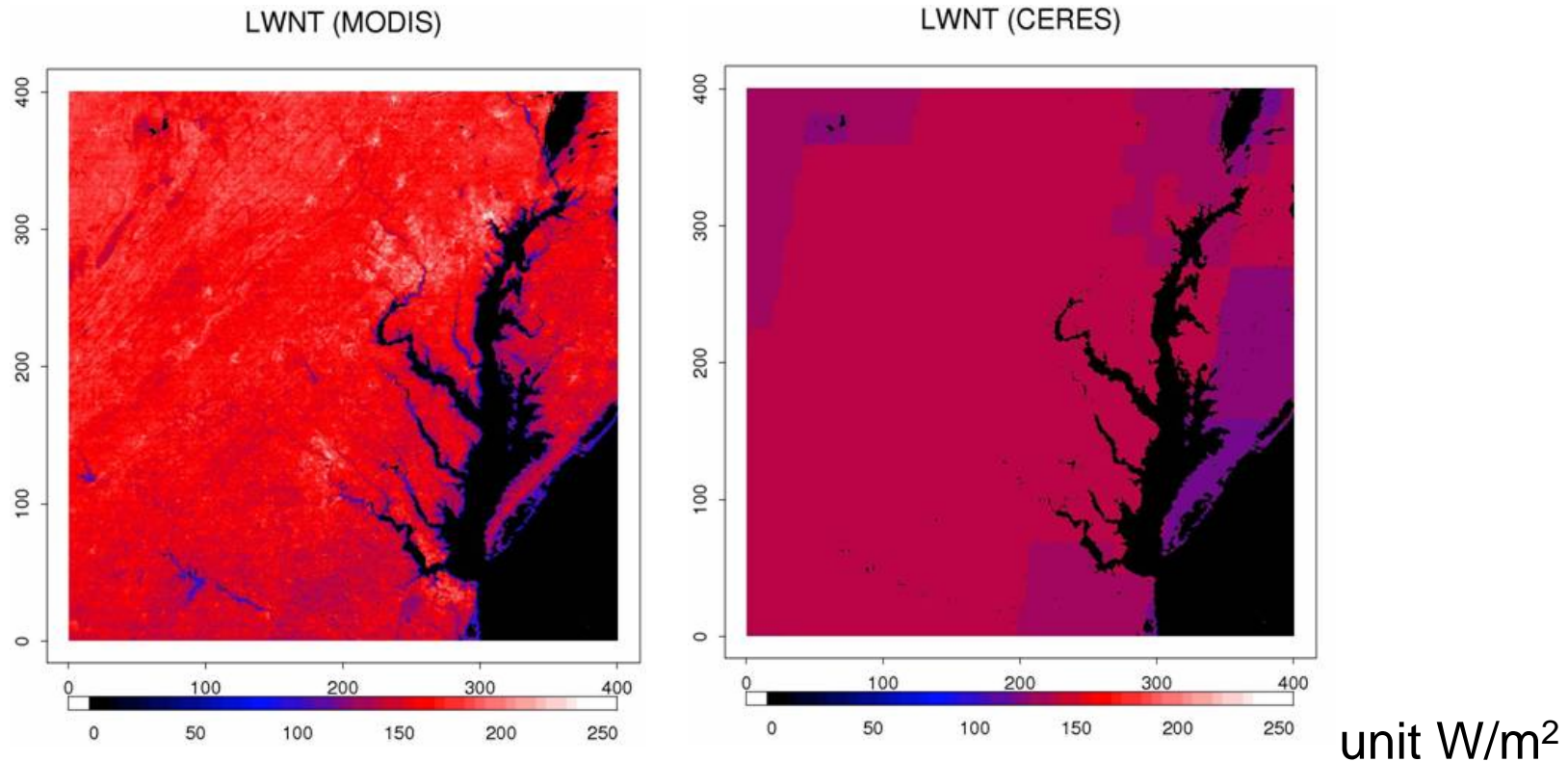
CERES:

derived from MODIS surface
temp. / emissivity products
(*Gupta et al., 1997*)

- MODIS: hybrid method

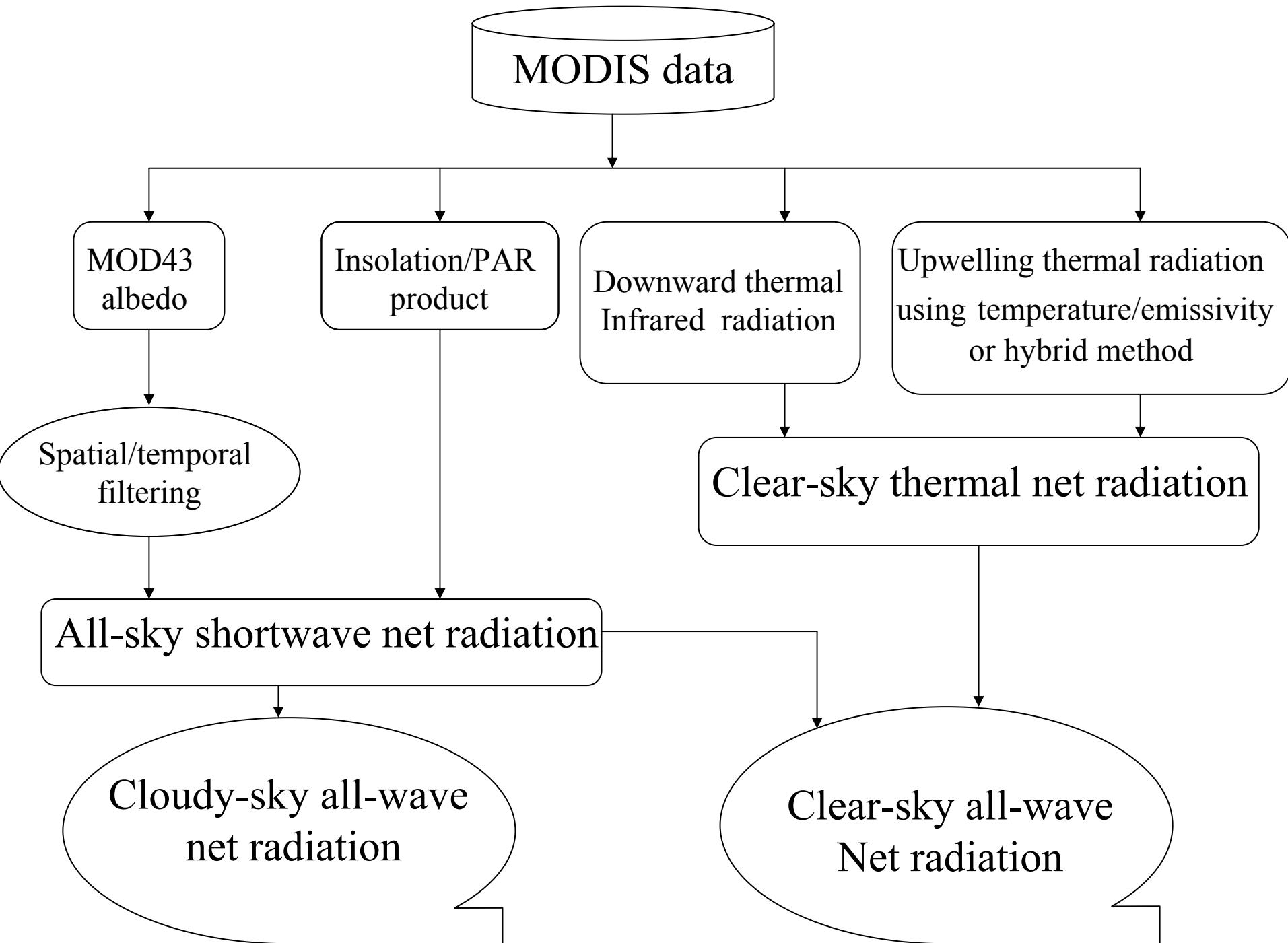
- SURFRAD validation
results: MODIS more
accuracy than CERES

Estimating LWNT



*MODIS-derived vs. CERES-derived instantaneous clear-sky
LWNT images over the Washington D.C. - Baltimore
Metropolitan Area (April 10, 2007 18:10 UTC, Aqua)*

- ♣ MODIS-derived LWNT: reveals more details
- ♣ MODIS LWNT $\sim 23 \text{ W}/\text{m}^2$ larger than CERES LWNT





Estimation of cloud-sky all-wave net radiation

Liang, et al.

Wang, K., & S. Liang, Estimation of Surface Net Radiation from Solar Shortwave Radiation Measurements, *Journal of Applied Meteorology and Climatology*, in press

An empirical formula to estimate surface daytime net radiation from solar shortwave radiation measurements and other meteorological products including daily minimum temperature, daily temperature range and relative humidity, and vegetation indices



UNIVERSITY OF
MARYLAND

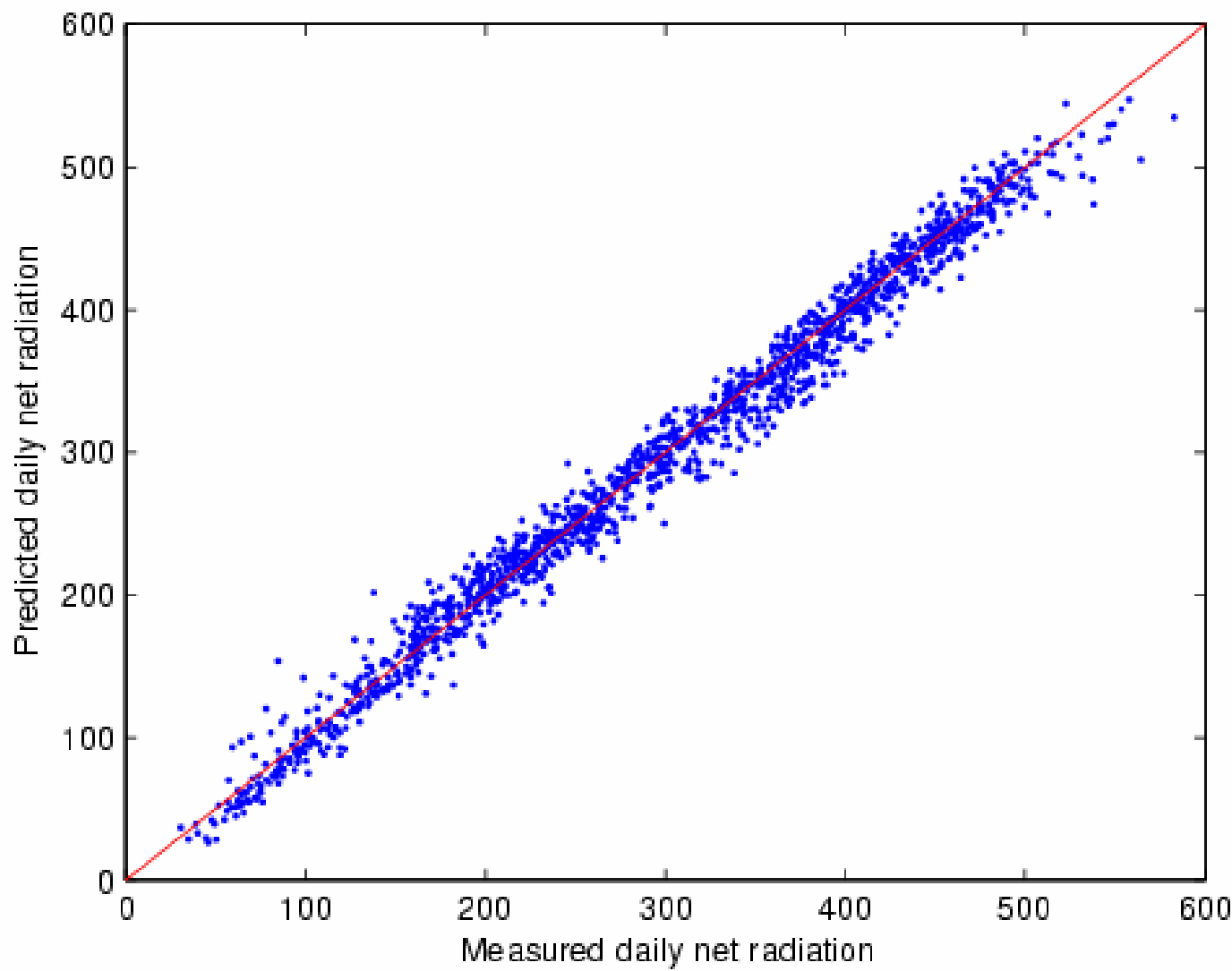


Figure 3. An example of scatterplots of measured and predicted daytime net radiation with Equations (5) and (6) using daily minimum land surface temperature, daily land surface temperature range, relative humidity and NDVI using data collected at Pawhuska, Oklahoma (EF12) from 2002 to 2006.



Summary

Liang, et al.

- ♣ Land surface radiation budget is highly related to global water cycle and carbon cycle;
- ♣ High spatial resolution net radiation product from polar-orbiting satellite observations is urgently needed for land applications;
- ♣ Algorithms have been developed to estimate surface radiation budget components from MODIS;
- ♣ Extensive validation activities are still needed for global product generation.



UNIVERSITY OF
MARYLAND



Liang, et al.

International Conference on Land Surface Radiation and Energy Budgets: Measurements, Modeling and Applications

Venue: Beijing Normal University

Date: March 18-20, 2009

Abstract due: Jan 15, 2009



Liang, et al.

Thank you !



UNIVERSITY OF
MARYLAND